

Science from LiteBIRD

LiteBIRD Collaboration: (François Boulanger, Martin Bucher, Erminia Calabrese, Josquin Errard, Fabio Finelli, Masashi Hazumi, Sophie Henrot-Versille, Eiichiro Komatsu, Paolo Natoli, Daniela Paoletti, Mathieu Remazeilles, Matthieu Tristram, Patricio Vielva, Nicola Vittorio)

8/11/2018

.....
The LiteBIRD satellite will map the temperature and polarization anisotropies over the entire sky in 15 microwave frequency bands. These maps will be used to obtain a clean measurement of the primordial temperature and polarization anisotropy of the cosmic microwave background in the multipole range $2 \leq \ell \leq 200$. The LiteBIRD sensitivity will be better than that of the ESA Planck satellite by at least an order of magnitude. This document summarizes some of the most exciting new science results anticipated from LiteBIRD. Under the conservatively defined “full success” criterion, LiteBIRD will measure the tensor-to-scalar ratio parameter r with $\sigma(r = 0) < 10^{-3}$, enabling either a discovery of primordial gravitational waves from inflation, or possibly an upper bound on r , which would rule out broad classes of inflationary models. Upon discovery, LiteBIRD will distinguish between two competing origins of the gravitational waves; namely, the quantum vacuum fluctuation in spacetime and additional matter fields during inflation. We also describe how, under the “extra success” criterion using data external to LiteBIRD, an even better measure of r will be obtained, most notably through “delensing” and improved subtraction of polarized synchrotron emission using data at lower frequencies. LiteBIRD will also enable breakthrough discoveries in other areas of astrophysics. We highlight the importance of measuring the reionization optical depth τ at the cosmic variance limit, because this parameter must be fixed in order to allow other probes to measure absolute neutrino masses. Other science includes cosmic birefringence, mapping the hot gas via the thermal Sunyaev-Zeldovich effect, anisotropic spectral distortions, polarization tests of possible anomalies in the temperature data, and Galactic Science.

1. Introduction

The LiteBIRD spacecraft [1–3] is designed to measure the temperature and polarization anisotropies of the cosmic microwave background (CMB) over the full sky in the multipole range $2 \leq \ell \leq 200$. LiteBIRD will map the entire sky in 15 microwave frequency bands from 34 to 448 GHz (with the band centers from 40 to 402 GHz). Such broad frequency coverage is indispensable for removing Galactic foreground emission at the level required to achieve LiteBIRD’s ambitious science objectives. Figure 1 shows the present state-of-the-art for measurements of the CMB temperature and polarization anisotropy power spectra. LiteBIRD will measure all these spectra, providing much improved measurements of the E- and B-mode polarization in the range $2 \leq \ell \leq 200$.

LiteBIRD was proposed to JAXA as a Strategic Large Mission in February 2015 and is currently undergoing a JAXA Phase A1 study. The baseline design consists of two telescopes [4]: a Low Frequency Telescope (LFT) and a High Frequency Telescope (HFT). Each telescope will use a rotating half-wave plate (HWP) polarization modulator as the first element

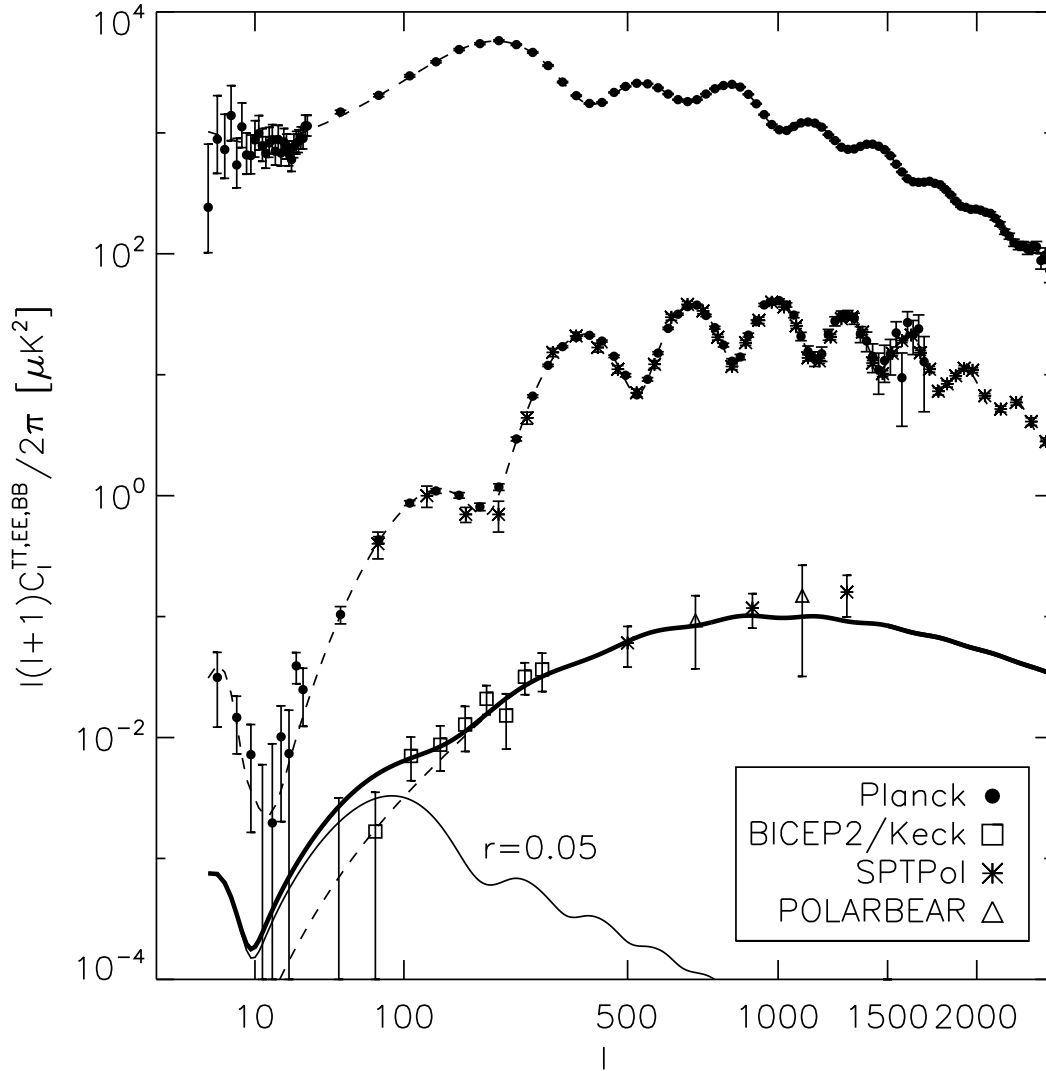


Fig. 1 CMB power spectra of the temperature anisotropy (top), E-mode polarization (middle), and B-mode polarization (bottom). The dashed lines show the best-fitting model for the scalar (density) perturbation, whereas the thin solid line at the bottom shows the prediction of a scale-invariant tensor (gravitational wave) perturbation with a tensor-to-scalar ratio parameter of $r = 0.05$, which is close to the current upper bound. The thick solid line shows the sum of two contributions to the B-mode polarization power spectrum: gravitational lensing (dashed line) and gravitational waves (thin solid line).

of its optical chain. Their focal planes [5, 6] will be cooled to 0.1 K and will be filled with several thousand transition edge sensor (TES) bolometers. Each pixel contains a broadband sinuous antenna coupled to the sky by a lenslet and measures several frequency bands simultaneously using a multi-choric technology. LiteBIRD will operate at the Sun-Earth Lagrange 2 (L2) point.

The full sky maps in 15 microwave bands will offer rich new data sets, which will enable exciting breakthroughs in a variety of science areas. In this document we shall describe new science involving: primordial gravitational waves from inflation (Sect. 2); the reionization of the Universe (Sect. 3); cosmic birefringence (Sect. 4); the hot gas in the Universe probed using the Sunyaev-Zeldovich effect (SZE; Sect. 5); spatially varying deviations from a perfect Planck blackbody CMB spectrum (Sect.6); tests with polarization of the so-called “anomalies” in the temperature data (Sect. 7); and Galactic science (Sect. 8).

Unlike LiteBIRD, the Planck satellite was not originally designed to measure polarization. As a consequence, the noise and systematic uncertainties in the polarization measurement are much greater than simplistic forecasts assuming only white noise would predict, especially at low ℓ . This explains why neither the Planck 2013 release nor the Planck 2015 release of cosmological results showed the polarization power spectrum for $\ell < 30$. Some partial results (in particular those pertaining to the reionization optical depth τ) were contained in the 2016 paper [7]). The final Planck 2018 release now contains the full Planck polarization results [8]. While Planck was not optimized for polarization, LiteBIRD uses a scanning pattern with near ideal cross-linking properties that serve to cancel systematic errors and optimize map making. Moreover, the presence of a rotating HWP allows for map making that does not rely on differencing measurements between different detectors, so that the map noise properties are close to the white noise limit. In short, LiteBIRD is optimized for polarization.

2. Primary science target: Primordial gravitational waves from inflation

2.1. *B-mode power spectrum*

The remarkable insight gained from cosmological research is that all cosmic structures, such as galaxies, stars, planets, and eventually us, probably originated from tiny quantum fluctuations in the early Universe. The wavelength of these initially microscopic quantum fluctuations was stretched by a quasi-exponential expansion known as “Cosmic Inflation” [9–14] by a factor of at least 10^{26} to macroscopic scales.¹ These quantum fluctuations served as the seeds of structure formation in the Universe [15–19]. Models of inflation based on a slowly rolling single scalar field predict a statistically homogeneous and isotropic, adiabatic, nearly Gaussian, and nearly scale-invariant spectrum of scalar curvature perturbations. All these predictions, including the deviation from an exactly scale invariant spectrum, have been confirmed by CMB data from the Wilkinson Microwave Anisotropy Probe (WMAP) [20], the Planck mission [21], and various ground-based observations [22–25]. Here “scale invariant spectrum” means that the variance of the perturbation is independent of wavelength λ . When the variance scales as λ^{1-n_s} , a scale invariant spectrum corresponds to $n_s = 1$.

These results provide strong evidence for inflation and for the quantum mechanical origin of cosmic structure. However, extraordinary claims require extraordinary evidence. Definitive evidence for inflation would come from the discovery of a stochastic background of gravitational waves [26–28]. Due to the inflationary expansion, the wavelength of these gravitational

¹ This estimate assumes that $V^{1/4} \approx 10^{16}$ GeV with a reheating temperature of order $T_{RH} \approx 10^{16}$ GeV, and if the scale of inflation is lower or reheating is at a lower temperature, this value can be lowered.

waves has been stretched to gigantic scales, e.g., billions of light years.² Such long wavelength gravitational waves cannot be generated by astrophysical sources such as binary black holes or neutron star mergers. These gravitational waves are a remarkable and unique prediction of inflation. Their detection would provide strong independent evidence for inflation, which some would argue would constitute the definitive confirmation of it.

Gravitational waves generate temperature anisotropies [29] as well as polarization anisotropies of the CMB [30, 31]. We can distinguish polarization generated by gravitational waves from those arising from sound waves (in this context also known as scalar perturbations) by comparing the symmetry of polarization patterns generated by these two sources. Sound waves generate only one type of polarization anisotropy (the E-mode), whereas gravitational waves generate both E-mode and B-mode polarization anisotropies [32, 33]. The middle dashed line in Fig. 1 shows the power spectrum of the E-mode polarization from sound waves, whereas the thin solid line in the bottom of the figure shows the B-mode polarization from primordial gravitational waves with $r = 0.05$, where r is the parameter that characterizes the amplitude of the gravitational waves and is called the “tensor-to-scalar ratio” parameter. This value is close to the current upper bound [34] of $r < 0.06$ (95 % C.L.). Throughout this document, we shall quote the tensor-to-scalar ratio and the tilt of the scalar power spectrum n_s at the wavenumber of 0.05 Mpc^{-1} .

LiteBIRD aims to detect and characterize the B-mode signal from gravitational waves by measuring the B-mode power spectrum over the multipole range $2 \leq \ell \leq 200$ (see Fig. 2). In particular LiteBIRD will be the only experiment likely able to access the predicted “re-ionization bump” in the B-mode power spectrum at $\ell \lesssim 10$, because measuring such low multipoles requires nearly full sky coverage and an exceedingly stable instrument to avoid systematic errors on large angular scales—in other words, a space mission.

2.2. Full success

A quantitative goal for the *full success* of LiteBIRD is to achieve a 68% CL uncertainty on the tensor-to-scalar ratio parameter of $\sigma(r = 0) < 10^{-3}$. Here $\sigma(r = 0)$ denotes the total uncertainty, including both statistical and systematic uncertainties when the true sky signal has no primordial gravitational waves, i.e., $r_{\text{true}} = 0$. This error budget includes foreground subtraction residuals.

Many inflationary models predict $r \geq 0.01$ [35]. In this case, LiteBIRD will be able to detect a signal at more than 10σ significance. The impact of such a discovery will be enormous. It would constitute direct evidence for cosmic inflation and would shed light on Grand Unified Theory (GUT) scale physics through the following relation between the inflaton potential V and the tensor-to-scalar ratio parameter r

$$V^{1/4} = (1.04 \times 10^{16} \text{ GeV}) \times \left(\frac{r}{0.01} \right)^{1/4}.$$

If the gravitational waves arise from the vacuum fluctuation in spacetime during inflation (see Sect. 2.4 for the other possible mechanisms), their detection will (arguably) mean the

²The standard prediction of single-field slow-roll inflation is a nearly scale-invariant spectrum of primordial gravitational waves (i.e., nearly equal amplitudes of gravitational waves at all scales from small to large). In this document we shall focus only on the gravitational waves accessible to the CMB observations, whose wavelength is of order billions of light years.

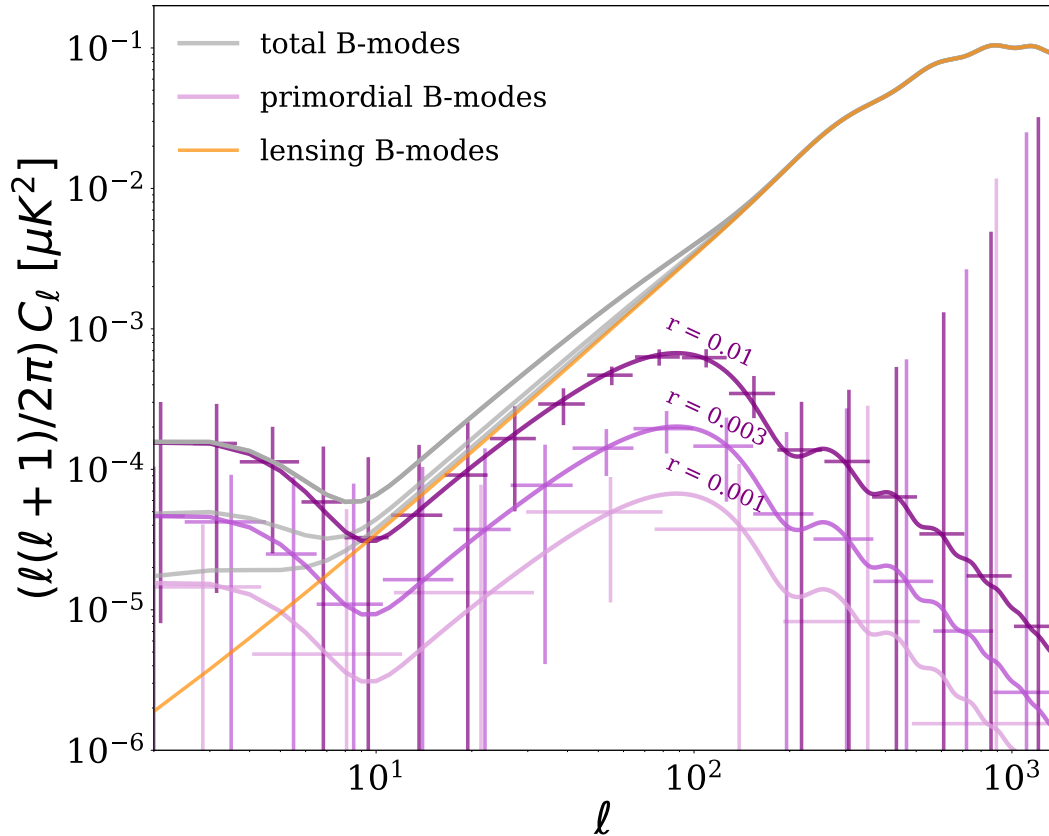


Fig. 2 B-mode power spectra from primordial gravitational waves (purple lines) and gravitational lensing (orange line), and the expected constraints from LiteBIRD (error bars). The top to bottom lines show $r = 0.01$, 0.003 , and 0.001 . The solid lines show the sums of the purple and orange lines. The error bars include instrumental noise, foreground residuals, and cosmic variance due to the primordial gravitational waves and gravitational lensing. No delensing has been performed.

first observation of quantum fluctuations of spacetime itself. If r is fairly large, this would establish a variation in the inflation field large compared to the Planck scale (i.e., so-called “large-field” inflation) [36]. This result would significantly constrain theories of quantum gravity such as superstring theories. We will be able to narrow down the region in the r vs. n_s plane of inflationary models allowed by the data (see the left panel of Fig. 3). If we do not detect a signal, LiteBIRD will set an upper limit of $r < 0.002$ at 95% C.L.

What would be the implication of such an upper bound? To answer this question, we focus on models with a small number of parameters. This is based on the Occam’s razor principle. In the history of physics, among many competing possibilities, the simplest and most elegant model has almost always won out. This experience supports using Occam’s razor as a guide. In our case, single-field slow-roll models are our targets. We can then use the following Lyth

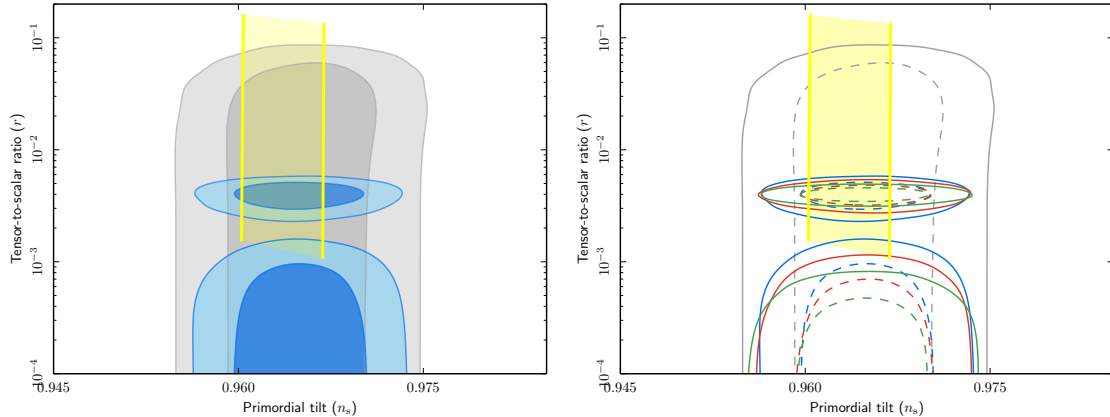


Fig. 3 (Left) Joint marginalized 68% and 95% CL constraints on the primordial tilt n_s and the tensor-to-scalar ratio r from LiteBIRD. The gray contours show the current limits. The top blue contours show the LiteBIRD constraints when the underlying inflationary model is a Starobinsky R^2 -like model [9] with $r_{\text{true}} = 0.004$, whereas the bottom contours show those for $r_{\text{true}} = 0$. The yellow band shows the predictions of the α -attractor class of inflationary models [37] for $\alpha > 1/3$. The Starobinsky model corresponds to $\alpha = 1$. (Right) Extra success (improved constraints on r) obtained by performing delensing with Planck CIB+WISE data (which already exists, denoted by the red lines), and with CIB+WISE combined with high-resolution ground-based CMB data at $3\mu\text{K}\cdot\text{arcmin}$, for example as from CMB Stage 4 (green lines). No delensing case is shown by the blue lines, which is the same as the contours in the left panel.

relation [36, 38]

$$r \approx 0.002 \left(\frac{60}{N} \right)^2 \left(\frac{\Delta\phi}{m_{pl}} \right)^2,$$

where N is the number of e -foldings, $\Delta\phi$ is the variation of the inflaton field during inflation, and m_{pl} is the reduced Planck mass. As long as this relation holds, we may conclude that LiteBIRD can rule out models with a large field variation, which are well-motivated phenomenologically. Note that the Lyth relation mentioned above is not an exact equation and there are models that violate the above relation even under the Occam's razor principle [39]. Model-dependent studies [39, 40], however, arrive at the same conclusion when we redefine $\Delta\phi$ as the characteristic scale of the inflaton field, which is defined as a range in which the inflaton potential changes in a significant way. See, for example, the detailed discussion is Section 2.5 of the CMB S4 Science Book [40], where a number of parametric models are analyzed as well as the references therein.

Consequently, LiteBIRD, with its $\sigma(r=0) < 10^{-3}$ or better sensitivity over $2 \leq \ell \leq 200$, would provide a fairly definitive statement about validity of the most important class of inflationary models, namely single-field slow-roll models with $\Delta\phi$ exceeding the Planck scale. Such a determination would constitute a milestone in cosmology.

Initially, when large-field inflationary models, which include $m^2\phi^2$, $\lambda\phi^4$, or more generally $V \sim M_{pl}^4(\phi/M_{pl})^n$, to give just a few examples, were in vogue, the expectation was that r would turn out to be relatively large. It was then believed that the detection of primordial

gravitational waves from inflation might lie just around the corner. But WMAP ruled out $\lambda\phi^4$ inflation at better than 99% confidence [41], a result confirmed and strengthened by Planck. The Planck data and combined with the BICEP2/Keck Array data have ruled out ϕ^4 inflation at approximately 7.5σ [21]. The Planck 2018 data combined with the BICEP2/Keck Array B-mode likelihood [42] suggest a preference for models with a concave downward or plateau-like potential [43]. This conclusion, however, is presently only a hint. Better experiments are needed to clarify the situation.

This tendency has inspired theorists to investigate how to motivate plateau-like potentials, both in the framework of effective field theory, and more ambitiously in the framework of string model building. An α -attractor family of models [37, 44–46] has been proposed in which a divergence in the Kähler potential yields a plateau whose shape is generic owing to the fact that the divergence in the Kähler metric blows up a minute part of the potential [47]. In these models inflation ends abruptly, in what figuratively might be described as a waterfall. This family is parameterized by α , where the $\alpha \rightarrow \infty$ limit connects with ϕ^2 inflation. Current work focuses on obtaining potentials of this sort within the framework of string model building (see for example [48] and references therein), and it is generally agreed that obtaining a small α is harder to achieve. This is, however, very much a current research topic, and at present definitive conclusions are lacking.

Other interesting models giving low values of r include the Starobinsky model [9], which interestingly was the first concrete model of inflation ever proposed, and Higgs inflation [49], where a non-minimal coupling to gravity flattens the potential at large field values [50]. For example, the Starobinsky model predicts $r = 12/N^2 = 0.004$ (with $N = 55$), which can be ruled out with more than a 3σ significance by LiteBIRD. These models are not exhaustive but simply serve to illustrate the present theoretical situation, which is developing. Interesting work has been carried out trying to elucidate the implications of the string landscape on the expectations for r . (See for example, Ref. [51] and references therein).

Perhaps the most important conclusion is that determining r observationally will have a tremendous impact by helping us understand how gravity unifies with the other three fundamental interactions, be it through string theory or through some other alternative theory of quantum gravity. Following on the success of the Standard Electroweak Model, whose correctness became more or less established in the early 1980s, this unification with gravity, presumably at around the Planck scale, has become the overarching goal of research in high energy theoretical physics.

Primordial gravitational waves are not the only source of B-mode polarization. Gravitational lensing of E-mode polarization generates B-mode polarization [52], which is shown as the bottom dashed line in Fig. 1. (The thick solid line shows the sum of the bottom thin solid and dashed lines.) While this signal offers a powerful probe of the growth of cosmic structure in a late time Universe, it also acts as “noise” for measurements of the primordial B-mode polarization. One can remove this signal (or “delens” [53, 54]) by measuring the matter distribution in the Universe, calculating the expected distortion in polarization maps, and removing the distortion from the maps. While delensing promises to reduce the statistical uncertainty in r , we do not use delensing information in defining the LiteBIRD criterion for the full success.

Polarized emission from our Galaxy (mostly synchrotron and thermal dust emission) and extra-galactic sources also generates B-mode polarization (e.g., [55]). We remove this “foreground emission” using the multi-frequency data of the LiteBIRD and by masking pixels at the locations of bright extra-galactic sources. The full success criterion includes the uncertainties induced by the foreground cleaning procedure.

2.3. *Extra success*

The full success criterion has been defined conservatively and does not rely on data external to LiteBIRD. Moreover, $\sigma(r=0)$ has been calculated including residuals from incomplete foreground removal. However, using external data, particularly in frequency bands below LiteBIRD’s lowest frequency band (at 34 GHz), will lead to smaller foreground residuals. External low-frequency ground-based data sets such as QUIJOTE [56, 57], C-BASS [58] and S-PASS [59] at frequency bands outside the LiteBIRD bands ($\nu < 34$ GHz) would be useful for potentially improved foreground cleaning and thus may contribute to “extra success.”

Another way to reduce $\sigma(r=0)$ is to “delens” using external data. Delensing removes the lensing B-modes by subtraction at the map level, thus reducing the lensing B-mode cosmic variance contribution described above rather than simply characterizing its power spectrum. Successful delensing using internal CMB data requires a higher angular resolution than that of LiteBIRD, because a low noise lensing reconstruction requires the imaging of a large number of small-scale modes.

However, there are several promising ways to delens LiteBIRD with external data and thus contribute to the extra success. Lensing measurements derived from ground-based CMB surveys, such as the CMB Stage 4 (CMB-S4) experiment and its precursors, can be used to substantially delens the LiteBIRD maps, reducing $\sigma(r)$ by 80% [corresponding to $f_{delens} = 0.1$] for CMB-S4. A less ambitious option would be to use Planck maps of the infrared background, along with the current Planck lensing and WISE data, to delens. Although this would give only a 45% reduction of $\sigma(r)$, corresponding to $f_{delens} = 0.57$, the data for such an analysis is already available. See the right panel of Fig. 3 for the expected improvements on the constraints in n_s - r space due to delensing.

Combining delensing and improved foreground cleaning with external data, it is reasonable to assume that we achieve $\sigma(r=0) < 0.0005$. In this case, we would be able to detect primordial gravitational waves with a significance of greater than 6σ if the Starobinsky model is correct.

2.4. *Beyond the B-mode power spectrum*

Single-field slow-roll inflation predicts that the stochastic background of gravitational waves originated from quantum fluctuations in spacetime generated during inflation. When we write the spatial metric (squared distance between two points in space) as

$$ds_3^2 = a^2(t) \sum_{ij} (\delta_{ij} + h_{ij}) dx^i dx^j ,$$

and impose the transverse traceless condition on h_{ij} , the matrix h_{ij} describes the “tensor” perturbations of the spatial metric. [$a(t)$ is the scale factor describing the expansion of the Universe, which grows exponentially in time during inflation.] When the wavelength of h_{ij}

is much smaller than the Hubble horizon size of the Universe, these metric perturbations propagate as gravitational waves.

Within the context of single-field slow-roll inflation, h_{ij} obeys the vacuum equation $\square h_{ij} = 0$. By quantizing this equation, we can show that a stochastic background of long-wavelength fluctuations of h_{ij} emerges with the following statistical properties:

1. A nearly scale invariant power spectrum (i.e., the tilt of the tensor power spectrum satisfies $n_t = -r/8$).
2. A nearly Gaussian probability distribution.
3. A parity-conserving probability distribution.

Detecting violation of any of these properties would point to new physics beyond the simplest minimal model. The first condition can be tested by reconstructing the power spectrum of h_{ij} from the B-mode power spectrum [60], the second by the three-point function (bispectrum) of h_{ij} [61–63], and the third by parity-violating correlation functions such as the cross-correlation between the temperature and the B-mode polarization and that between the E- and B-mode polarizations [64].

These conditions can be violated when other fields are present during inflation. They provide an additional source of gravitational waves: $\square h_{ij} = -16\pi G\pi_{ij}$, where π_{ij} is the tensor component of the stress-energy tensor of the other fields. These fields must have sub-dominant energy density compared to the main scalar field driving inflation (inflaton). However, they can still contribute an energy density sufficient to produce a gravitational wave with an amplitude large enough to be detected by LiteBIRD.

What are these fields? They could be scalar fields [65–68], a U(1) gauge field [69–73], or a non-Abelian SU(2) gauge field [74–79]. All these sources can produce strongly scale-dependent gravitational waves that are highly non-Gaussian, while the latter two sources can produce parity-violating gravitational waves. Thus *all* the above conditions can be violated. If the gravitational waves sourced by the right-hand side of the wave equation dominate over those from the left-hand side (i.e., the vacuum fluctuation in the spatial metric), detecting a B-mode polarization from primordial gravitational waves does *not* imply the discovery of the quantum nature of space. (But such a discovery would still provide definitive evidence for inflation because we need inflation to stretch the wavelength of gravitational waves to billions of light years.)

An example of a U(1) gauge field is the primordial magnetic field, which can source tensor perturbations that are non-scale-invariant, non-Gaussian, and parity-violating. Magnetic fields can also induce a spatially-dependent rotation of polarization angles of the CMB by means of Faraday rotation (e.g., [80]). The effect can be detected using multi-frequency data because the Faraday rotation angle is proportional to ν^{-2} .

It is of the utmost importance to confirm the above three properties of h_{ij} using the LiteBIRD data before claiming discovery of the quantum nature of spacetime. If we discovered violation of any of the above properties from LiteBIRD, it would have profound implications on our understanding of the new physics at play during inflation.

3. Optical depth and reionization of the Universe

The hydrogen atoms in the intergalactic medium are fully ionized in the recent Universe (for $z < 6$). We have multiple evidence for this fact from the lack of saturated hydrogen

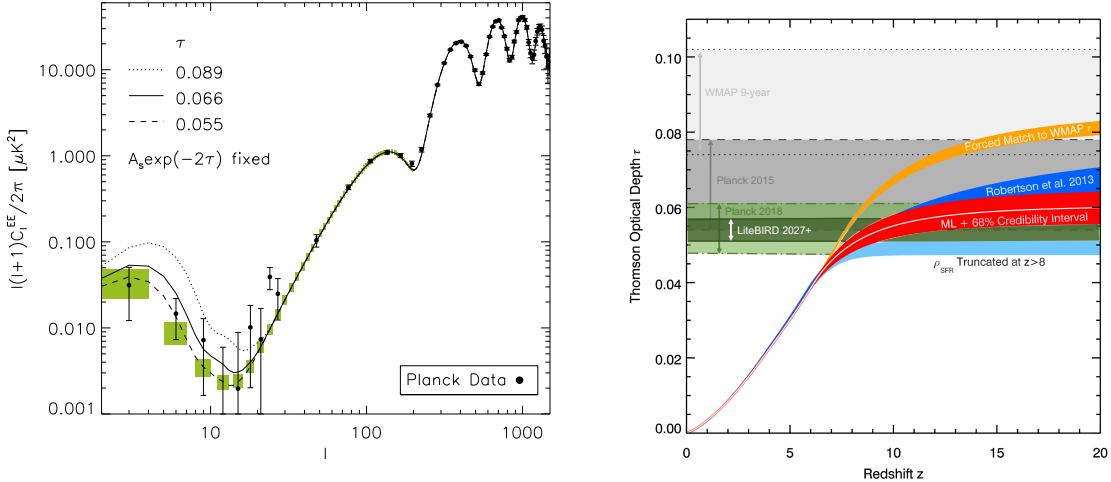


Fig. 4 (Left) E-mode power spectrum with the optical depths of $\tau = 0.089$ (WMAP 9-year [86]; dotted), 0.066 (Planck 2015 with LFI polarization and CMB lensing [87]; solid), and 0.055 (Planck with HFI polarization [88]; dashed). We vary the primordial scalar curvature amplitude such that the product $A_s \exp(-2\tau)$ is fixed. The green boxes show the expected LiteBIRD constraints at $\ell = 2 - 200$, binned with $\Delta\ell = 3$. (Right) Optical depths predicted from various models of the number counts of star forming galaxies, as a function of the maximum redshift z (re-adapted from [89]). The green band shows the expected LiteBIRD 68% and 95% CL constraints on τ . The other bands show the WMAP and Planck constraints.

absorption lines in spectra of quasars and gamma ray bursts (Gunn-Peterson test) [81–85]. Given that the Universe became almost completely neutral after hydrogen recombination (at $z \approx 1000$), the Universe must have “reionized” during some intermediate epoch.

While astrophysics of reionization is not well understood, there are several ways to observe this epoch: the number counts of star-forming galaxies and quasars at $z > 6$, which were presumably producing ionizing photons [89]; redshifted 21-cm lines from hydrogen atoms before the completion of reionization [90]; Doppler shifts of CMB photons by the bulk motion of ionized gas [91] (called the kinetic Sunyaev-Zeldovich effect [92]); and finally, the polarization of the CMB produced by electrons scattering quadrupole temperature anisotropies in a reionized Universe [93].

Electrons in a reionized Universe see the quadrupole temperature anisotropy from *their own* last scattering surface due to the polarization dependence of Thomson scattering. Consequently, these anisotropies scattered by electrons in turn produce a polarization of the CMB, which we can observe today [94]. The amplitude of the polarization is proportional to the optical depth to electron scattering τ . The wavenumber of the fluctuations contributing to quadrupole temperature anisotropy as seen by an electron at a redshift z is given by $k \approx 3/[r_L - r(z)]$ where $r_L = 14$ Gpc is the comoving distance to our last-scattering surface, and $r(z)$ is the comoving distance to the redshift z . For example, a redshift of $z = 7.7$ gives $r(7.7) = 9.1$ Gpc. We observe this wavenumber at a multipole of $\ell \approx kr(7.7) \approx 6$, which corresponds to the so-called “reionization bump” in the polarization power spectra. The effect on the E-mode is shown in the left panel of Fig. 4.

The height of the reionization bump is proportional to $\tau^2 A_s$ where A_s is the amplitude of the scalar curvature power spectrum. On the other hand, scattering washes out small-scale power by $\exp(-2\tau)$; thus, for a given high- ℓ power spectrum, the height of the reionization bump scales as $\tau^2 \exp(2\tau) \approx \tau^2(1 + 2\tau)$. We can use this to determine the value of τ , which in turn provides an integrated constraint on the reionization history of the Universe because $\tau = \sigma_T N_e$ where the column density of electrons is given by $N_e = c \int dt n_e$ integrated from today to the beginning of reionization. This number can be compared with the expected number of electrons from ionization by star-forming galaxies and quasars (see the right panel of Fig. 4).

Measuring the reionization optical depth precisely is challenging because of the foreground contamination that must be accurately removed and moreover because of systematic uncertainties, which are most problematic on very large angular scales where most of the statistical information concerning τ is situated. The value of τ evolved from the value of $\tau = 0.177^{+0.08}_{-0.07}$ from the WMAP first-year analysis [95] using the TE cross-relation power spectrum at low- ℓ to the final combined polarization and temperature observations from the WMAP 9-year observations gave $\tau = 0.089 \pm 0.014$ [86]. The Planck 2013 Planck release [96] did not use the EE data to constrain τ because of difficulties in understanding and removing systematic errors, although the Planck 2015 release did give a value of τ based on the low- ℓ LFI 70 GHz polarization map giving $\tau = 0.067 \pm 0.023$ and $\tau = 0.078 \pm 0.019$ when combined with data at higher ℓ [45]. However, in this Planck 2015 analysis the more sensitive HFI maps at 100 and 143 GHz were not used. In the final, Planck 2018 analysis [8], including all the frequencies a value of $\tau = 0.054 \pm 0.007$ is cited. All the above values are at 68% C.L. It is, however, difficult to assess the reliability of this determination as the Planck 2018 Likelihood paper has not yet been released. Weiland et al. [97], for example, argue that $\tau = 0.07 \pm 0.02$ represents a more conservative estimate of the current state-of-the-art of our knowledge of τ . It seems likely that the current measurements may not be the last word on this important parameter.

LiteBIRD will provide a cosmic variance limited determination of τ (i.e., the smallest possible error bar limited only by the fraction of sky available for the cosmological analysis f_{sky}). For the fiducial value of $\tau = 0.06$ and the sky fraction of $f_{\text{sky}} = 0.7$, the expected 68% CL cosmic variance on τ is 0.002 [98], which is 6 times better than 2016 error bars [88] and 3.5 times better compared to the latest claim [99]. Not only is this a significant improvement over the current measurement, but it will also be the definitive and accurate measurement of τ . The report from the External International Science Review for LiteBIRD states: “*A cosmic variance limited measurement of EE on large angular scales will be an important, and guaranteed, legacy for LiteBIRD.*”

One important motivation to determine τ more accurately is the quest to determine the sum of the neutrino masses [101, 102], in particular in order to distinguish the inverted neutrino mass hierarchy (i.e., two heavy, one light) from the normal hierarchy. Massive neutrinos slow down structure formation [103]. Consequently, we can measure the neutrino mass by comparing the amplitude of fluctuations in the low redshift Universe with that at the last scattering surface (i.e., A_s). However, we cannot determine A_s unless we know τ . Thus, improved τ from LiteBIRD will play a major role in measuring the neutrino mass. For

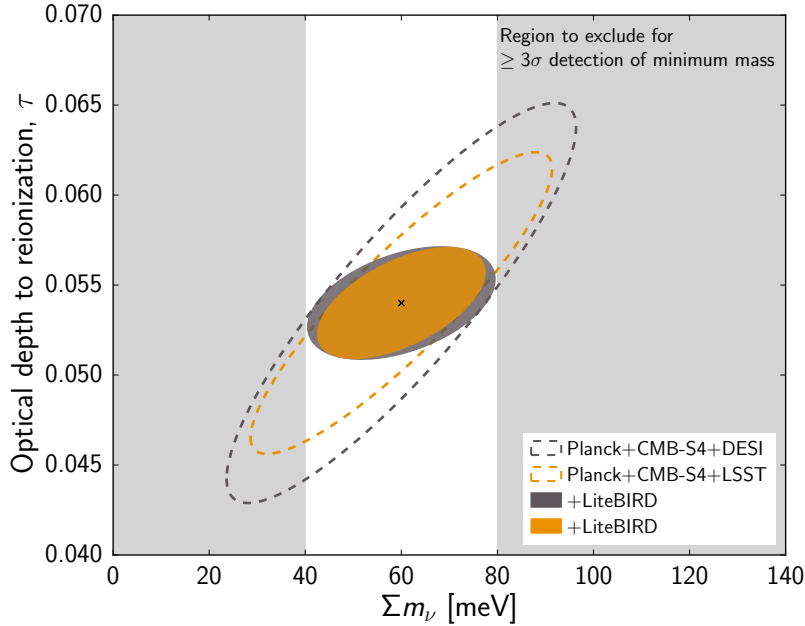


Fig. 5 Two-dimensional marginalized contour levels at 68% C.L. for the optical depth to reionization and the sum of the neutrino masses as measured by future combinations of CMB and large-scale structure data (for example including BAO from DESI or galaxy lensing and clustering from LSST). The contours are centered on the fiducial values $\tau = 0.054$ and $\Sigma m_\nu = 60$ meV as indicated by the cross. A cosmic variance limited measurement of τ is reached with LiteBIRD [i.e., $\sigma(\tau) = 0.002$]. This τ limit will enable a better neutrino mass measurement, reaching a 5σ detection when combined with DESI or LSST. The shaded gray region shows the Σm_ν 1-dimensional marginalized area to be excluded around the fiducial model in order to achieve a detection of significance greater than 3σ , thus highlighting the importance of including LiteBIRD data in the analysis. [Figure adapted from Ref. [100].]

example, LiteBIRD’s τ measurement would reduce the uncertainty in the neutrino mass by more than a factor of two (see the Appendix of [102]).

This new measurement of the optical depth, when combined with CMB lensing data from the future CMB-S4 experiment and data from large scale structure surveys tracing the matter distribution (for example, the baryon acoustic oscillation (BAO) data from the DESI galaxy survey [104] or galaxy lensing/clustering data from the LSST survey [105]), will also enable a $\geq 3\sigma$ cosmological detection of the sum of neutrino masses, even for the minimum, 60 meV sum of masses [106]. Figure 5 shows that a cosmic variance limited measurement of τ from LiteBIRD will be necessary to reach a significant detection of the neutrino mass from cosmological data.

To complete the picture on the neutrino sector, the expected error bar on the effective number of relativistic species, N_{eff} , from LiteBIRD alone is of the same order of magnitude as the one obtained by Planck [107]. Still, it would give an independent measurement, and an important cross-check, as it has been shown for instance in [108] that the N_{eff} value depends on the modelling of the foregrounds in the high- ℓ Planck likelihoods. More accurate

value of N_{eff} would also help constrain the energy density of the stochastic gravitational wave background Ω_{GW} [109], as the gravitational waves behave as radiation.

Beyond a cosmic variance limited measurement of the optical depth, the E-mode measurements by LiteBIRD constrain the precise reionization history [110]. In particular, the ‘‘dip’’ in the E-mode power spectrum at $\ell \approx 20$ in Fig. 4 can distinguish between instantaneous reionization at a redshift of z_{reion} and a reionization history extending to $z > z_{\text{reion}}$. A recent analysis [111] shows that an extended reionization history out to $z \gtrsim 10$ may be preferred by the Planck data at the 95% CL. The LiteBIRD data can provide a definitive test of this extended reionization history [112–114]. The discussion above supposes homogeneous reionization; however, reionization is in fact expected to be patchy and LiteBIRD will be able to characterize this patchiness [115].

4. Cosmic birefringence

If the new physics that generated the initial scalar (curvature) and tensor (gravitational wave) fluctuations does not violate parity (or spatial inversion) symmetry and the CMB photons do not experience any parity-violating processes as they propagate to us today, any parity-violating correlation functions such as the temperature-B-mode correlation (TB correlation) and the EB correlation must vanish. This is because under spatial inversion, the spherical harmonic coefficients transform as follows:

$$\begin{aligned} a_{\ell m}^T &\rightarrow +(-1)^\ell a_{\ell m}^T, \\ a_{\ell m}^E &\rightarrow +(-1)^\ell a_{\ell m}^E, \\ a_{\ell m}^B &\rightarrow -(-1)^\ell a_{\ell m}^B. \end{aligned} \tag{1}$$

Consequently, the expectation value of any parity odd observable, such as the TB or EB correlations, must vanish if the underlying physics is parity conserving. If the underlying physics violates parity, these correlation functions can and generically do have non-vanishing expectation values.

We discussed the TB and EB correlations induced by parity-violating gravitational waves from gauge fields in Sect. 2.4. (Also see ref. [116] for a different mechanism to produce parity-violating gravitational waves.) In this section we describe an effect known as ‘‘cosmic birefringence’’ [117, 118]. The basic idea is that a new parity-violating coupling of a scalar field to the electromagnetic tensor rotates the direction of the polarization as the CMB photons propagate through space. In other words, space filled with this scalar field behaves as if it were a birefringent medium, hence the name ‘‘cosmic birefringence.’’ See ref. [119, 120] for a summary of the current constraints on birefringence.

A homogeneous scalar field coupled to the electromagnetic field via the Chern-Simons term rotates the polarization direction uniformly over the sky by an angle $\Delta\alpha$, converting E-mode polarization into B-mode polarization. We would therefore observe a B-mode polarization even if initially there were no B-mode polarization. The measured power spectra $C_\ell^{XY,\text{obs}}$ are related to the intrinsic spectra according to (see [121])

$$\begin{aligned} C_\ell^{TE,\text{obs}} &= C_\ell^{TE} \cos(2\Delta\alpha), \\ C_\ell^{TB,\text{obs}} &= C_\ell^{TE} \sin(2\Delta\alpha), \\ C_\ell^{EE,\text{obs}} &= C_\ell^{EE} \cos^2(2\Delta\alpha), \\ C_\ell^{BB,\text{obs}} &= C_\ell^{EE} \sin^2(2\Delta\alpha), \end{aligned}$$

$$C_\ell^{EB,\text{obs}} = \frac{1}{2} C_\ell^{EE} \sin(4\Delta\alpha),$$

and for $\Delta\alpha \ll 1$ this becomes

$$\begin{aligned} C_\ell^{TB,\text{obs}} &= (2\Delta\alpha) C_\ell^{TE}, \\ C_\ell^{EB,\text{obs}} &= (2\Delta\alpha) C_\ell^{EE}, \\ C_\ell^{BB,\text{obs}} &= (2\Delta\alpha)^2 C_\ell^{EE}. \end{aligned}$$

Unfortunately, this effect is completely degenerate with an instrumental miscalibration of polarization angles by $\Delta\alpha$. Since such miscalibration generates a spurious B-mode power spectrum of $C_\ell^{BB,\text{obs}} = (2\Delta\alpha)^2 C_\ell^{EE}$, we must calibrate the angles with a precision sufficient to achieve $\sigma(r=0) < 10^{-3}$. However, there are no strong polarized astrophysical sources in the sky with precisely known polarization angles. Consequently, the calibration must rely on the measurements on the ground, which limits the accuracy of calibration to a bit better than 1 degree, which is much larger than the requirement of order 0.05 degree. One could also consider launching a small satellite carrying a polarized light source to the L2 for the calibration purpose. How well this strategy works in practice is still under study. As a result, the option of using the TB and EB correlations (assumed to vanish) to calibrate the instrumental polarization angles [122] constitutes the present baseline. This method works because we have an accurate knowledge of the cosmological TE and EE power spectra from sound waves, and it is straightforward to fit to the TB and EB power spectra to solve for $\Delta\alpha$ with arcmin precision.

While this “self-calibration” procedure eliminates LiteBIRD’s sensitivity to uniform rotation caused by a scalar field, we can still look for an *anisotropy* in $\Delta\alpha$ [123, 124]. This introduces correlations between T and B and between E and B at different multipoles, [i.e., $\langle a_{\ell m}^T a_{\ell' m'}^E \rangle$ and $\langle a_{\ell m}^E a_{\ell' m'}^B \rangle$], in a manner similar to gravitational lensing [125, 126]. This property makes it possible to create a map of $\Delta\alpha$ in each LiteBIRD pixel. This map will be useful not only for probing new parity-violating physics, but also for characterizing instrumental systematics.

The primordial magnetic field also generates spatially-varying $\Delta\alpha$ via the Faraday rotation, which has been constrained by the ground-based experiments [127, 128]. LiteBIRD can improve the limit on the amplitude of a nearly scale-invariant primordial magnetic field by an order of magnitude [80].

On the other hand, TB and EB correlations from parity-violating gravitational waves can easily be distinguished from angle miscalibration because the shape of TB and EB power spectra from gravitational waves is different from that arising from rotation of the scalar perturbations [64] (see Fig. 6).

5. Mapping the hot gas in the Universe

Electrons in the hot ionized gas transfer their energy to CMB photons by inverse Compton scattering, leading to a characteristic distortion of the blackbody spectrum of the CMB (see Fig. 7). This phenomenon is known as the thermal SZE [129, 130] and has been routinely detected toward the directions of galaxy clusters [131–134]. The amplitude of the thermal SZE is given by the so-called “Compton y parameter,” which is given by $\tau k_B T_e / m_e c^2$ where τ is the optical depth and T_e and m_e are the electron temperature and mass, respectively.

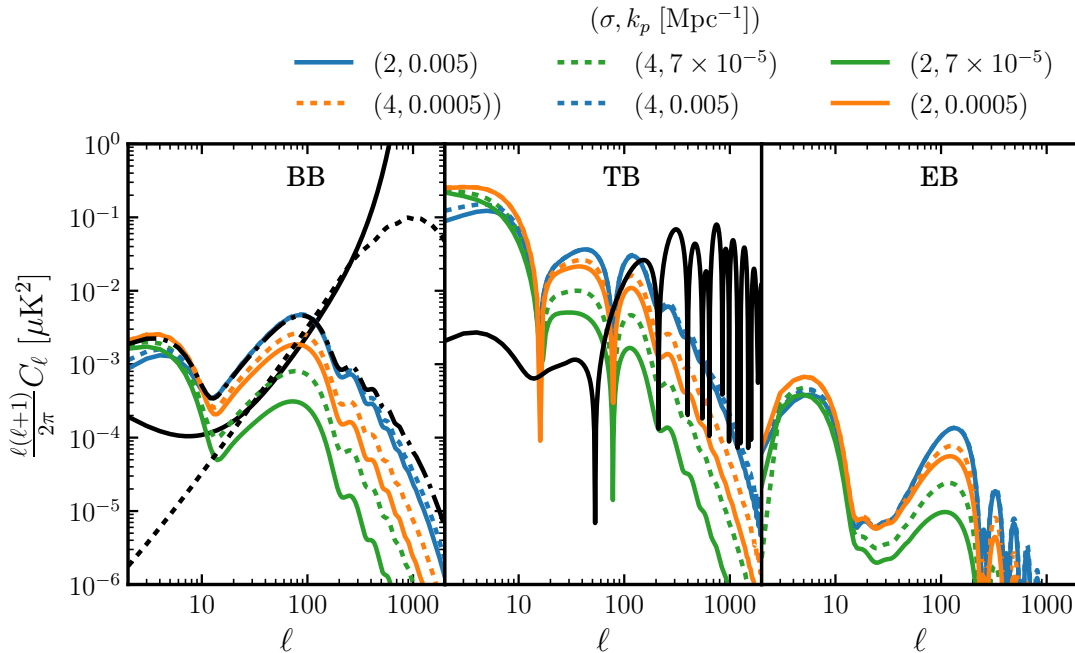


Fig. 6 B-mode power spectra (left) and TB (middle) and EB (right) power spectra from gauge fields during inflation [64]. The lines with different colors show BB, TB, and EB spectra with various combinations of the model parameters. The black solid line in the left panel shows the LiteBIRD noise power spectrum with 2% residual foreground contamination, while the dotted line shows the lensing B-mode power spectrum. The dash-dotted line shows the B-mode power spectrum from a scale-invariant gravitational wave with a tensor-to-scalar ratio parameter of $r = 0.07$. The black line in the middle panel shows the TB power spectrum from instrumental miscalibration of polarization angles by one arcminute. Similarly, in the right panel the miscalibration would show up as the E-mode power spectrum in figure 1 times $2\Delta\alpha$, which can be distinguished easily from the signals shown here.

Using the so-called Needlet Internal Linear Combination (NILC) [135, 136], we can reconstruct an all-sky map of thermal SZE and its angular power spectrum with minimum residual foreground contamination [137]. Applying the same component separation algorithm that was used on the Planck data to the LiteBIRD simulations, we find that while the Planck SZE map still contains contamination from various foreground sources due to the limited number of frequency bands, LiteBIRD can faithfully reconstruct the tSZ map at $\ell > 10$. See Fig. 8 for the power spectrum of the reconstructed SZE map from the simulation.

Exploiting the 15 LiteBIRD frequency bands will yield a much improved, high-fidelity SZE map over the full sky at $\ell \leq 200$ essentially free of contamination. This full sky map will show in projection all hot gas in the Universe and will have a lasting impact on astrophysics as legacy data from LiteBIRD. An important application of this full sky thermal SZE map will be to cross-correlate with a full sky three-dimensional catalogue of galaxies, as discussed in [138].

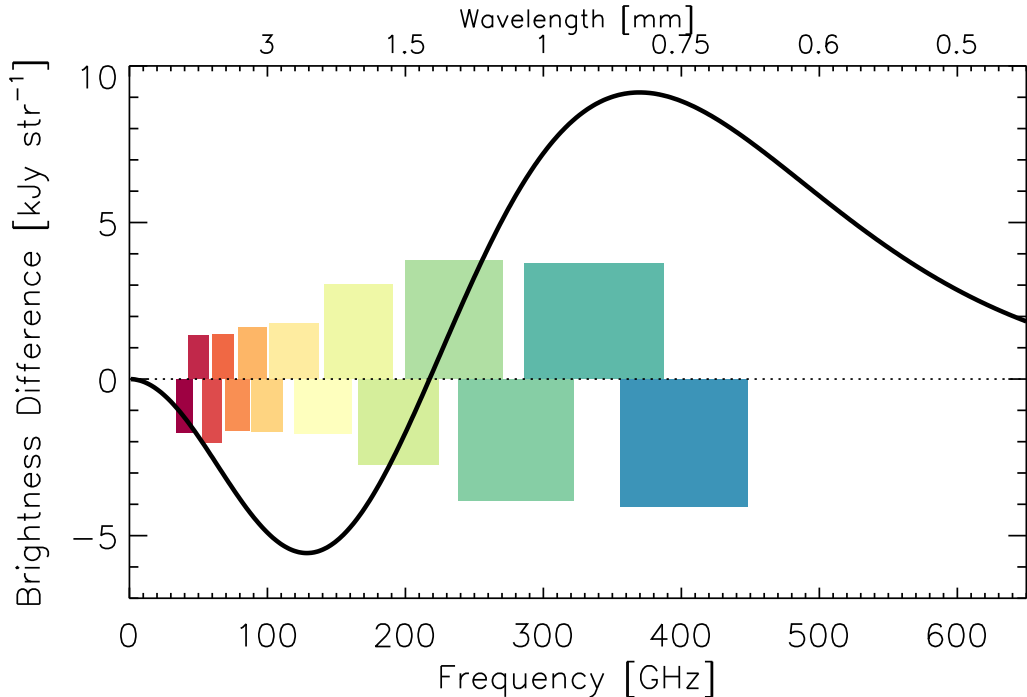


Fig. 7 Spectrum of the thermal SZE (solid line). The shape of the spectrum is universal in the limit of $k_B T_e / m_e c^2 \ll 1$ while its amplitude depends on the Compton y parameter. We use $y = 5 \times 10^{-6}$. The color bars show the sensitivity of the 15 partially overlapping bands of the LiteBIRD detectors in units of kJy str^{-1} . For clarity we show half of bands as positive and the other half as negative values, but only their absolute values are meaningful.

Figure 7 shows the SZE spectrum in the non-relativistic limit (where $k_B T_e / m_e c^2 \ll 1$). Its shape is universal and depends only on the mean CMB temperature. However, small relativistic corrections to this shape are proportional to $k_B T_e / m_e c^2$. Detecting this relativistic correction averaged over a full sky SZE map can yield the mean gas temperature of the Universe, providing an “integral constraint” on physics of the intergalactic medium [139] and stringent and robust constraints on the energy feedback from supernovae and active galactic nuclei (AGNs).

6. Anisotropic CMB spectral distortions

Although LiteBIRD is not sensitive to the uniform (monopole) component of spectral distortion (compared to a perfect Planck blackbody CMB spectrum), LiteBIRD is very sensitive to the spatially varying component of the spectral distortion. The thermal SZE described in Sect. 5 is an example of such a spectral distortion and can be used to map the distribution of hot gas in the Universe.

Early on, when the temperature of the Universe exceeded five million K (or $z > 2 \times 10^6$ in terms of redshift), double Compton scattering (which changes the total photon number) was efficient in relaxing photon spectrum to a Planck spectrum with vanishing chemical potential, even if extra energy was injected into the plasma [140, 141]. If however energy is injected between $5 \times 10^4 < z < 2 \times 10^6$, double Compton scattering is no longer fast enough to relax

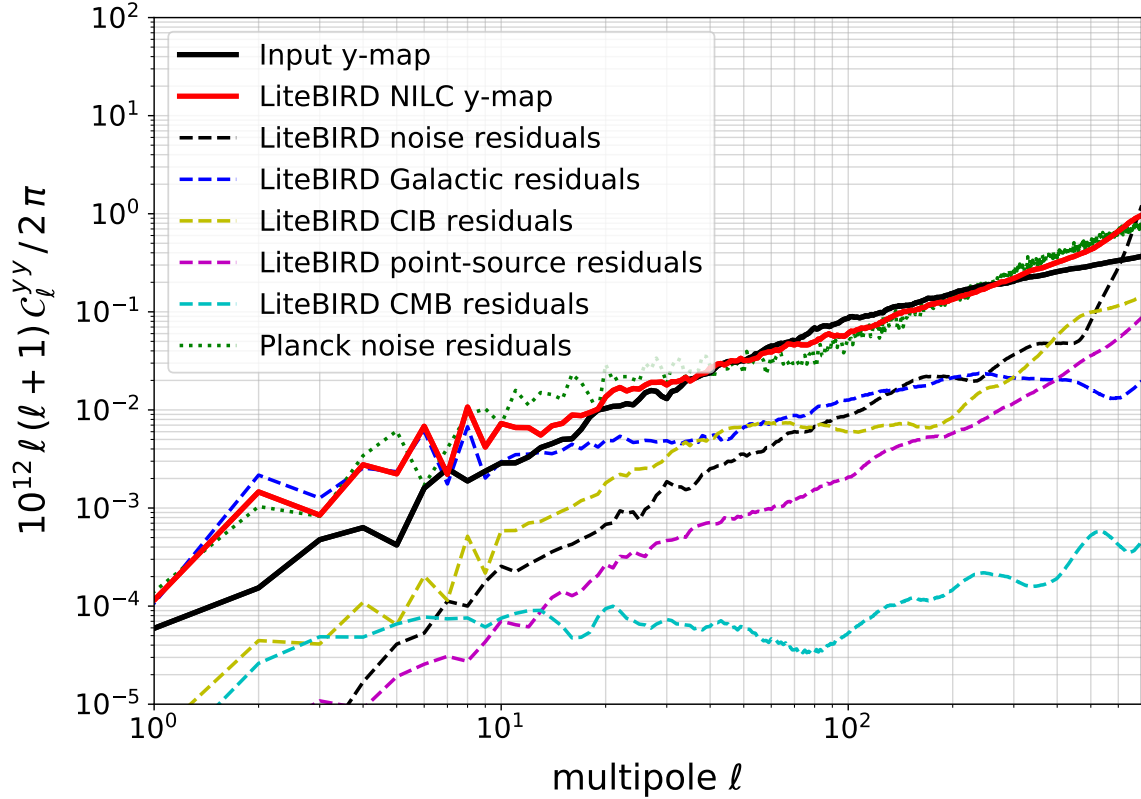


Fig. 8 Reconstructed power spectrum of the thermal SZE from the LiteBIRD simulation (red line), compared with the input one (black line). Both agree well except at $\ell < 10$, which still shows the residuals of the Galactic emission; however, such low multipoles suffer from large non-Gaussian cosmic variance error bars. The noise power spectrum of LiteBIRD (black dashed line) is much lower than that of Planck (green dotted line), showing substantially improved sensitivity and fidelity of the thermal SZE map of LiteBIRD.

the photon spectrum to a Planck spectrum with no chemical potential. However, Compton scattering is still efficient for re-distributing the photon energies so as to maintain an equilibrium distribution (i.e., a Bose-Einstein distribution with *non-zero* chemical potential, also known as μ distortion). The spectral distortion caused by energy injection after $z = 5 \times 10^4$, however, does not relax to an equilibrium distribution because the energy exchange due to Compton scattering becomes inefficient, resulting in, for example, a permanent spectrum distortion such as the SZE described in Sect. 5.

While there exist many theoretical possibilities for energy injection in the early Universe before $z = 5 \times 10^4$ (see refs. [142, 143] for reviews), one mechanism present in the Standard Model of Cosmology is energy injection from the dissipation of sound waves [144, 145]. As the spectral distortion occurs at second order in the perturbation, the energy injection rate due to the dissipation of sound waves is proportional to the sound wave amplitude squared. This property makes it possible to constrain the small-scale power of fluctuations from the chemical potential [146–148].

While this signal is isotropic in the sky if the fluctuations obey Gaussian statistics, a specific type of non-Gaussian fluctuations called “squeezed non-Gaussianity” can be produced

by certain physical mechanisms during inflation such as multi-field effects and non-Bunch-Davies vacuum initial conditions and would generate spectral distortions characterized by a *spatially varying* chemical potential [149, 150]. LiteBIRD can look for this signal by cross-correlating the measured temperature anisotropies with a map of chemical potential reconstructed from LiteBIRD’s multi-frequency data, as this cross-correlation measures a three-point function (temperature fluctuation on large scales correlated with the amplitude of sound waves squared on small scales). While the multi-field effect of inflation yields only a small signal-to-noise ratio for LiteBIRD given the constraints on this type of non-Gaussianity from Planck data [151], non-vacuum effect can yield a large signal-to-noise ratio, offering a powerful test of physics of inflation at its onset [150].

Light axion-like particles convert into photons in the presence of magnetic fields, generating anisotropic distortions in the CMB spectrum [152]. In particular, “resonant conversion” of axions into photons by the Galactic magnetic field yields *polarized* spectral distortion of the CMB with the spatial distribution of the signal tracking the Galactic magnetic field. Thus LiteBIRD can look for this signal.

7. Elucidating anomalies with polarization

The overarching narrative of the Planck analysis has been to emphasize how well the six-parameter ‘concordance’ model can explain the data [8, 45, 96]. It is doubtless a triumph that a simple model can account for the data. We are, however, plagued with a number of “tensions” or “anomalies” at modest statistical significance (i.e., $2\text{--}3\sigma$) [see refs. [153, 154] and references therein for a discussion], which can reasonably be interpreted either as statistically insignificant, or alternatively as interesting hints of new physics, which theorists should endeavor to explain.

Given the high stakes, we cannot content ourselves with proclaiming prematurely that concordance is the end of the story. We must carry out the best possible tests to shed as much light as possible on whether these anomalies are real. Planck has explored these anomalies almost at the cosmic variance limit in temperature but not in polarization. By providing low- ℓ E-mode polarization maps dominated by cosmic variance, LiteBIRD will almost double the statistical information concerning these anomalies.

We now describe some of the most important anomalies on which LiteBIRD may be expected to provide significant new data:

(1) Low- ℓ power deficit

Fig. 9 taken from the Planck 2018 release shows the observed temperature anisotropy compared to the concordance model with the best-fitting parameters. Below are shown the residuals. Because of the large cosmic variance at low ℓ , the multipoles with $\ell \lesssim 30$ have little pull on the cosmological parameters, of which there are six in the concordance model. The cosmological parameters, and in particular the amplitude A_s and spectral index n_s , are almost completely determined by the observations at large ℓ , and the same would hold for the running of the spectral index if added as an extra parameter. The open question is whether the concordance model can explain the low ℓ observations. We observe a dip at around $\ell \approx 20$ and more generally a deficit in power for $\ell < 30$.

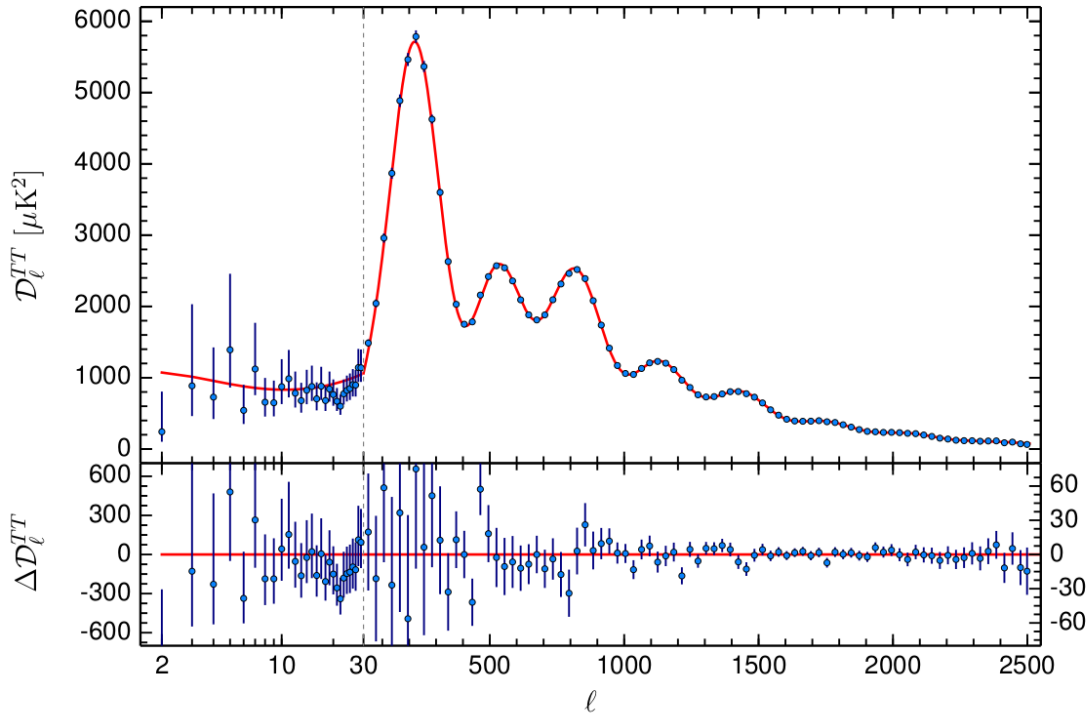


Fig. 9 Low- ℓ power spectrum anomalies from the Planck 2018 temperature power spectrum [8]. The upper panel shows the zoom-in of the Planck 2018 temperature power spectrum shown in Fig. 1 with the concordance model prediction using best-fitting parameters (red curve). The lower panel shows the residuals to this fit. While at high ℓ the fit is good, at low ℓ there are signs of a power deficit, with the possibility of a dip around $\ell \approx 20$.

Is this simply a statistical fluke, or is it an error in the measurements, possibly from some systematic, or oversubtracted foregrounds (where part of the primordial signal has been mistaken for foreground contamination)? Given the analysis, the latter explanations seem unlikely. The likelihood of observing this anomaly as a result of chance within the concordance model depends somewhat on what estimator is used, and one must also account for the look-elsewhere effect, but the significance is modest—somewhere in the neighborhood of 2σ .

(2) Hemispherical asymmetry

Hemispherical asymmetry, or dipolar modulation, is the simplest possible model under which the underlying statistical process generating the primordial perturbations might not be the same in all directions. Almost all theoretical models—or, more precisely, all the simplest theoretical models—predict that the same power spectrum should be measured in different patches of the sky (up to differences plausibly attributable to cosmic variance).

Current CMB data indicate that the power spectra as measured on opposite hemispheres differ to a degree unlikely to be explained by cosmic variance alone, although the statistical significance of this result is modest [153, 155]. This anomaly was first noted by WMAP [156, 157], but because of the absence of high frequency dust channels for the WMAP experiment, it was in principle possible that the anomaly might

somehow result from inadequate Galactic dust emission modelling. Planck was able to test this explanation thanks to its high frequency channels, and was also able to search for dipolar modulation on smaller angular scales, where in the simplest models one would expect a signal with much higher signal-to-noise. The Planck results ruled out the possibility that the WMAP result could be a dust artifact, and more interestingly showed that the signal for a modulation was present only for $\ell \lesssim 64$, contrary to the predictions of the simplest models.

Although the Planck team also looked for dipolar modulation in polarization, the constraints using polarization are much weaker than the cosmic variance limit. LiteBIRD will be able to provide cosmic variance limited E mode data to enable the ultimate assessment of the statistical evidence for dipolar modulation as well as other models violating the assumption of isotropy of the underlying stochastic process generating the primordial cosmological perturbations. See Ref. [158] for a discussion of the even-odd anomaly and forecasts of how new better polarization data could potentially increase its statistical significance.

(3) **Axis of evil**

It has been pointed out that a number of low- ℓ temperature multipoles line up to define a common axis in a manner very unlikely to occur under the assumption of an isotropic Gaussian stochastic process [159]. Several authors have sought to explain these coincidences, for example by means of considering anisotropic cosmological models. Are these coincidences simply a statistical fluke, or are they a hint of new physics beyond the concordance model? This question is difficult to answer as we have a natural tendency to find patterns, and unlike in laboratory experiments, we cannot fix our estimator and then accumulate more data to see whether the anomaly persists. Fortunately, we can look to see whether the same axes are also found in the polarization.

(4) **Cold spot**

After smoothing the cleaned primordial CMB temperature map over various scales, the maxima and minima of the map can be compared to expectations assuming a Gaussian underlying theory. This exercise carried out using a 400 arcminute smoothing kernel yields a “cold spot,” which is expected to occur in slightly less than 1% of the maps generated using a Gaussian process with the same power spectrum (where no attempt has been made to include the look-elsewhere effect). See [153] and references therein. LiteBIRD will tell us whether polarization anomalies occur at the same location as the cold spot.

To the above anomalies we should also add tensions with non-CMB determinations of the cosmological parameters. One example is the measurement of the present value of the Hubble constant H_0 . The Planck 2018 Cosmological Parameters paper reports the determination $H_0 = 67.4 \pm 0.5 \text{ km s}^{-1} \text{ Mpc}^{-1}$, which conflicts with the determination using more traditional methods (i.e., based on surveying the low- z universe by establishing a “cosmic distance ladder”, etc.) obtaining $73.45 \pm 1.66 \text{ km s}^{-1} \text{ Mpc}^{-1}$ [160]. These two results disagree at the level of 3.3σ . Since this tension is modest, one could argue that at this point at least we should not worry too much. However, this tension could also be the hint of new physics.

It is significant that these two kinds of measurements are vulnerable to completely different types of errors. On the one hand, the CMB H_0 determination crucially relies on the assumption that the six-parameter concordance model correctly describes the physics at play when the CMB anisotropies were imprinted. Small corrections or extensions to the concordance model would shift the determination of H_0 and affect the estimation of its error. On the other hand, the low- z measurements of H_0 do not rely on knowing the correct model for the early universe processes. These measurements, however, suffer from other uncertainties, for example in the corrections from galactic dust extinction and the modelling of variable stars and supernovae. Measurements of H_0 by surveying the low- z universe will improve as new infrared observations, for which there is virtually no extinction, come online, as well as better determinations using independent techniques such as water masers, gravitational waves, and gravitational lensing. It will also be important to improve the error bars on the CMB side with better E mode polarization data limited only by cosmic variance. LiteBIRD has an important contribution to make in this endeavor.

8. Galactic science

Cosmic magnetism remains an unresolved puzzle of fundamental importance to astrophysics. Magnetic fields are ubiquitous. Yet little is known regarding their origin and the dynamo processes believed to have amplified a weak initial seed field and maintained their strength through cosmic time [161].

The role that magnetic fields play in the evolution of the universe also remains an important open question. As has often been the case in astrophysics, our understanding extrapolates from observations of the very local universe, from the Milky Way and nearby galaxies. Magnetic fields have been shown to play an important role in the dynamics and evolution of the Milky Way. A better understanding of magnetic fields would enable progress to be made in understanding the astrophysics of galaxies. Examples include the dynamics and energetics of the multiphase interstellar medium (ISM), star formation efficiency, the acceleration and propagation of cosmic rays, and the impact of feedback on galaxy evolution.

Magnetic fields are not only critical to understanding galaxies. The magnetized ISM in the solar neighborhood poses an obstacle to investigation of cosmic signals. Dust and synchrotron emission from the Galaxy contaminate measurements of CMB polarization [162] and CMB spectral distortions [163]. The Galactic ISM complicates investigating the 21cm line emission of neutral hydrogen from Cosmic Dawn and the Epoch of Reionization [164] as well as of extragalactic magnetic fields [165]. Galactic magnetic fields also prevent us from identifying the sources of ultra-high energy cosmic rays [166].

A broad range of science objectives cannot be achieved unless there is progress in modeling the Galactic magnetic fields, which in turn motivates ambitious efforts to acquire relevant data [167]. As a result, Galactic Magnetism is today an extremely active research field, driven by the rapid advances in observational capabilities.

Observations of the Galactic polarization were among the most interesting outcomes of the Planck space mission. Spectacular images combining the intensity of dust emission with the texture derived from polarization data have received worldwide attention and have become part of the general scientific culture [168]. Beyond this popular impact, the Planck polarization maps have represented a great leap forward for Galactic astrophysics [169]. We anticipate a comparable contribution from LiteBIRD. LiteBIRD will provide full sky maps of dust

polarization at sub-mm wavelengths with a sensitivity many times better than the Planck 353 GHz polarization map. Such maps can be obtained only from a space mission. This data will complement the rich array of polarization observations including stellar polarization surveys to be combined with Gaia astrometry [170], and synchrotron observations together with Faraday rotation measurements at radio wavelengths with the Square Kilometer Array and its precursors [171]. Here we sketch two main directions of research.

8.1. *Magnetic fields*

Dust polarization probes the magnetic field orientation in dusty regions, mostly in the cold and warm neutral phases of the ISM, which account for the bulk of the gas mass, and hence also of the dust mass. These ISM phases include self-gravitating gaseous structures within star forming molecular clouds and account for the bulk of the turbulent gas kinetic energy [172]. Thus among the various means available to map the structure of interstellar magnetic fields, dust polarization is best suited to trace the dynamical interplay between magnetic fields, turbulence, and gravity in the ISM. This interplay is pivotal to star formation. It is also central to cosmic magnetism because it constrains the interplay between magnetic fields and the formation of structures in the universe across cosmic time and scales [161].

The multiphase magnetized ISM is too complex to be described by an analytic theory. Our understanding in this research field follows from observations, numerical magnetohydrodynamic (MHD) simulations, and phenomenological models. A wealth of spectroscopic observations of gas species tracing the gas density, its column density and its kinematics obtained from ground telescopes is available. LiteBIRD will provide complementary data with comparable statistics regarding magnetic fields.

LiteBIRD observations at the highest frequency (i.e., 402 GHz) will improve on the Planck 353 GHz sensitivity to dust polarization by a factor 50, increasing the number of modes measured over the sky by a comparable factor. While the analysis of dust polarization at high Galactic latitude is limited today by the Planck sensitivity to an effective angular resolution $\sim 1^\circ$, LiteBIRD will extend this resolution to its $10'$ beam size at 402 GHz. The LiteBIRD 402 GHz polarization map will become the new reference for the statistical analysis of magnetic fields and their correlation with the matter and gas kinematics, in the neutral, atomic, and molecular ISM phases.

This improvement in sensitivity will open new research directions that one cannot fully anticipate. Moreover, this new data will further the characterization of the correlation between magnetic fields and the filamentary structure in the diffuse ISM and star forming clouds [173, 174]. More generally, LiteBIRD will provide the data statistics required to explore the non-Gaussianity (intermittency) of magnetic fields, and to uncover coherent magnetic structures, arising from the nonlinear interplay between turbulent gas motions and magnetic fields, and the dissipation of turbulence [175, 176]. Our current knowledge derives from MHD simulations that lack the dynamic range needed to explore the full range of scales of interstellar turbulence [177]. The LiteBIRD data will be crucial to test how well MHD simulations agree with the observed behavior of astrophysical plasmas.

8.2. *Interstellar dust*

The analysis of the LiteBIRD data will also include the spectral characterization of Galactic polarization. The current description of the Galactic contribution to the Planck and WMAP polarization data as arising from two components, namely dust thermal emission and synchrotron [162, 178], is likely to prove inadequate for LiteBIRD. LiteBIRD will provide data at 15 frequency bands between 40 and 402 GHz with a sensitivity a factor of 15 to 50 times better than the corresponding frequencies of Planck and WMAP. This significantly better sensitivity may lead to discoveries concerning the dust composition and the physics of grain alignment.

Interstellar dust is often modeled as a mixture of silicate and carbon grains. If silicates contain magnetic inclusions, or if the interstellar dust includes free flying magnetic grains, Galactic polarization may include a significant contribution from magnetic dipole emission [179]. Dipole emission from spinning dust grains is thought to account for the anomalous microwave emission (AME)³ but the nature of the carriers remains uncertain [180]. The competing hypotheses, namely polycyclic aromatic hydrocarbons, small silicates, and magnetic nanoparticles, differ in their predictions for the AME polarization. A detection of AME polarization will thus constrain the nature of its carriers. The current limit on AME polarization from the diffuse ISM is set by the cross-correlation between the dust and synchrotron polarization [181]. Comparing level of the cross-correlation of the low frequency LiteBIRD maps with dust to the cross-correlation with dust of the synchrotron maps from observations from the ground at even lower frequencies (e.g., the C-Band all-sky survey at 5 GHz [182]) promises to establish new constraints on the polarization of the AME, because these lower frequency maps are virtually free of AME.

The emission properties of dust at long wavelengths have been shown by Planck to vary throughout the ISM [183, 184]. Likewise, the alignment efficiency depends on both the local physical conditions and the dust composition [185]. Variations in both dust properties and alignment efficiency are likely to be correlated with the density structure of the ISM, which in turn is known to be correlated with the magnetic field structure. These correlations are expected to violate the simplest assumption for component separation under which the spectral frequency dependence of the Galactic polarization and its angular structure on the sky factorize. This effect, known as frequency decorrelation, has not yet been detected by Planck [162]. However it is likely that LiteBIRD will encounter this additional complexity. Frequency decorrelation complicates the separation of the Galactic and primordial CMB polarizations. We will need to understand and characterize this new complexity in order to assess its impact on the search for primordial B-modes. This aspect of the data analysis will also contribute to update and test models of dust emission and of grain alignment, which are of interest for the interpretation of dust polarization data.

Acknowledgments

EK thanks Glenn Starkman for discussions on the implications of the E-mode polarization data on the low correlation in the temperature data. We would like to thank Bruce Draine,

³ If the AME is rotational emission, the grains must have sizes < 1 nm in order to contribute a significantly to the observed signal.

Katia Ferrière, Brandon Hensley, Kazunori Kohri, Eric Linder, Isabelle Ristorcelli, and Blake Sherwin for useful discussions and invaluable comments.

References

- [1] M. Hazumi et al., Proc. SPIE Int. Soc. Opt. Eng., **8442**, 844219 (2012).
- [2] T. Matsumura et al., J. Low. Temp. Phys., **176**, 733 (2014), arXiv:1311.2847.
- [3] H. Ishino et al., Proc. SPIE Int. Soc. Opt. Eng., **9904**, 99040X (2016).
- [4] H. Sugai et al., Proc. SPIE Int. Soc. Opt. Eng., **9904**, 99044H (July 2016).
- [5] T. Matsumura et al., J. Low. Temp. Phys., **184**(3-4), 824–831 (2016).
- [6] A. Suzuki et al. (2018), arXiv:1801.06987.
- [7] Planck Collaboration Int. XLVII, Astronomy and Astrophysics, **596**, A108 (December 2016), 1605.03507.
- [8] Planck Collaboration VI (2018), arXiv:1807.06209.
- [9] A. A. Starobinsky, Phys. Lett., **91B**, 99–102 (1980).
- [10] K. Sato, Mon. Not. Roy. Astron. Soc., **195**, 467–479 (1981).
- [11] A. H. Guth, Phys. Rev., **D23**, 347–356 (1981).
- [12] A. Albrecht and P. J. Steinhardt, Phys. Rev. Lett., **48**, 1220–1223 (1982).
- [13] A. D. Linde, Phys. Lett., **108B**, 389–393 (1982).
- [14] A. D. Linde, Phys. Lett., **129B**, 177–181 (1983).
- [15] V. F. Mukhanov and G. V. Chibisov, JETP Lett., **33**, 532–535, [Pisma Zh. Eksp. Teor. Fiz.33,549(1981)] (1981).
- [16] A. A. Starobinsky, Phys. Lett., **117B**, 175–178 (1982).
- [17] S. W. Hawking, Phys. Lett., **115B**, 295 (1982).
- [18] A. H. Guth and S. Y. Pi, Phys. Rev. Lett., **49**, 1110–1113 (1982).
- [19] J. M. Bardeen, P. J. Steinhardt, and M. S. Turner, Phys. Rev., **D28**, 679 (1983).
- [20] E. Komatsu et al., PTEP, **2014**, 06B102 (2014), arXiv:1404.5415.
- [21] Planck Collaboration XX, Astron. Astrophys., **594**, A20 (2016), arXiv:1502.02114.
- [22] K. T. Story et al., Astrophys. J., **779**, 86 (2013), arXiv:1210.7231.
- [23] J. L. Sievers et al., JCAP, **1310**, 060 (2013), arXiv:1301.0824.
- [24] K. Aylor et al., Astrophys. J., **850**(1), 101 (2017), arXiv:1706.10286.
- [25] T. Louis et al., JCAP, **1706**(06), 031 (2017), arXiv:1610.02360.
- [26] L. P. Grishchuk, Sov. Phys. JETP, **40**, 409–415, [Zh. Eksp. Teor. Fiz.67,825(1974)] (1975).
- [27] A. A. Starobinsky, JETP Lett., **30**, 682–685, [Pisma Zh. Eksp. Teor. Fiz.30,719(1979)] (1979).
- [28] L. F. Abbott and Mark B. Wise, Nucl. Phys., **B244**, 541–548 (1984).
- [29] R. K. Sachs and A. M. Wolfe, Astrophys. J., **147**, 73–90 (1967).
- [30] A. G. Polnarev, Sov. Astron., **29**, 607–613 (1985).
- [31] R. Crittenden, R. L. Davis, and P. J. Steinhardt, Astrophys. J., **417**, L13–L16 (1993), arXiv:astro-ph/9306027.
- [32] U. Seljak and M. Zaldarriaga, Phys. Rev. Lett., **78**, 2054–2057 (1997), arXiv:astro-ph/9609169.
- [33] M. Kamionkowski, A. Kosowsky, and A. Stebbins, Phys. Rev. Lett., **78**, 2058–2061 (1997), arXiv:astro-ph/9609132.
- [34] Keck Array and BICEP2 Collaborations: PAR Ade et al., ArXiv e-prints (October 2018), 1810.05216.
- [35] Marc Kamionkowski and Ely D. Kovetz, Ann. Rev. Astron. Astrophys., **54**, 227–269 (2016), arXiv:1510.06042.
- [36] David H. Lyth, Phys. Rev. Lett., **78**, 1861–1863 (1997), arXiv:hep-ph/9606387.
- [37] Renata Kallosh, Andrei Linde, and Diederik Roest, JHEP, **11**, 198 (2013), arXiv:1311.0472.
- [38] Paolo Creminelli, Diana L. López Nacir, Marko Simonović, Gabriele Trevisan, and Matias Zaldarriaga, JCAP, **1511**(11), 031 (2015), arXiv:1502.01983.
- [39] Andrei Linde, JCAP, **1702**(02), 006 (2017), arXiv:1612.00020.
- [40] Kevork N. Abazajian et al. (2016), arXiv:1610.02743.
- [41] E. Komatsu et al., Astrophys. J. Suppl., **180**, 330–376 (2009), arXiv:0803.0547.
- [42] P. A. R. Ade et al., Phys. Rev. Lett., **116**, 031302 (2016), arXiv:1510.09217.
- [43] Planck Collaboration X (2018), arXiv:1807.06211.
- [44] John Joseph M. Carrasco, Renata Kallosh, and Andrei Linde, JHEP, **10**, 147 (2015), arXiv:1506.01708.
- [45] Planck Collaboration XIII, Astron. Astrophys., **594**, A13 (2016), arXiv:1502.01589.
- [46] Renata Kallosh, Andrei Linde, and Diederik Roest, JHEP, **08**, 052 (2014), arXiv:1405.3646.
- [47] Ewan D. Stewart, Phys. Rev., **D51**, 6847–6853 (1995), arXiv:hep-ph/9405389.
- [48] C. P. Burgess, M. Cicoli, S. de Alwis, and F. Quevedo, JCAP, **1605**(05), 032 (2016), arXiv:1603.06789.
- [49] F. Bezrukov, A. Magnin, M. Shaposhnikov, and S. Sibiryakov, JHEP, **01**, 016 (2011), arXiv:1008.5157.
- [50] Eiichiro Komatsu and Toshifumi Futamase, Phys. Rev., **D59**, 064029 (1999), arXiv:astro-ph/9901127.

-
- [51] Georges Obied, Hiroshi Ooguri, Lev Spodyneiko, and Cumrun Vafa (2018), arXiv:1806.08362.
- [52] M. Zaldarriaga and U. Seljak, *Phys. Rev.*, **D58**, 023003 (1998), arXiv:astro-ph/9803150.
- [53] J. Carron, A. Lewis, and A. Challinor, *JCAP*, **1705**(05), 035 (2017), arXiv:1701.01712.
- [54] A. Manzotti et al., *Astrophys. J.*, **846**(1), 45 (2017), arXiv:1701.04396.
- [55] BICEP2/Keck Array and Planck Collaborations, *Phys. Rev. Lett.*, **114**, 101301 (2015), arXiv:1502.00612.
- [56] R. Génova-Santos et al., *Mon. Not. Roy. Astron. Soc.*, **452**(4), 4169–4182 (2015), arXiv:1501.04491.
- [57] R. Génova-Santos et al., *Mon. Not. Roy. Astron. Soc.*, **464**(4), 4107–4132 (2017), arXiv:1605.04741.
- [58] M. O. Irfan et al., *Mon. Not. Roy. Astron. Soc.*, **448**, 3572–3586 (April 2015), 1501.06069.
- [59] N. Krachmalnicoff et al. (2018), arXiv:1802.01145.
- [60] Takashi Hiramatsu, Eiichiro Komatsu, Masashi Hazumi, and Misao Sasaki, *Phys. Rev.*, **D97**(12), 123511 (2018), arXiv:1803.00176.
- [61] M. Shiraishi, C. Hikage, R. Namba, T. Namikawa, and M. Hazumi, *Phys. Rev.*, **D94**(4), 043506 (2016), arXiv:1606.06082.
- [62] Aniket Agrawal, Tomohiro Fujita, and Eiichiro Komatsu, *Phys. Rev.*, **D97**(10), 103526 (2018), arXiv:1707.03023.
- [63] Aniket Agrawal, Tomohiro Fujita, and Eiichiro Komatsu, *JCAP*, **1806**(06), 027 (2018), arXiv:1802.09284.
- [64] B. Thorne, T. Fujita, M. Hazumi, N. Katayama, E. Komatsu, and M. Shiraishi, *Phys. Rev.*, **D97**(4), 043506 (2018), arXiv:1707.03240.
- [65] J. L. Cook and L. Sorbo, *Phys. Rev.*, **D85**, 023534, [Erratum: *Phys. Rev.*D86,069901(2012)] (2012), arXiv:1109.0022.
- [66] D. Carney, W. Fischler, E. D. Kovetz, D. Lorshbough, and S. Paban, *JHEP*, **11**, 042 (2012), arXiv:1209.3848.
- [67] M. Biagetti, M. Fasiello, and A. Riotto, *Phys. Rev.*, **D88**, 103518 (2013), arXiv:1305.7241.
- [68] L. Senatore, E. Silverstein, and M. Zaldarriaga, *JCAP*, **1408**, 016 (2014), arXiv:1109.0542.
- [69] L. Sorbo, *JCAP*, **1106**, 003 (2011), arXiv:1101.1525.
- [70] M. M. Anber and L. Sorbo, *Phys. Rev.*, **D85**, 123537 (2012), arXiv:1203.5849.
- [71] N. Barnaby and M. Peloso, *Phys. Rev. Lett.*, **106**, 181301 (2011), arXiv:1011.1500.
- [72] N. Barnaby, J. Moxon, R. Namba, M. Peloso, G. Shiu, and P. Zhou, *Phys. Rev.*, **D86**, 103508 (2012), arXiv:1206.6117.
- [73] M. Peloso, L. Sorbo, and C. Unal, *JCAP*, **1609**(09), 001 (2016), arXiv:1606.00459.
- [74] A. Maleknejad and M. M. Sheikh-Jabbari, *Phys. Lett.*, **B723**, 224–228 (2013), arXiv:1102.1513.
- [75] E. Dimastrogiovanni and M. Peloso, *Phys. Rev.*, **D87**(10), 103501 (2013), arXiv:1212.5184.
- [76] P. Adshead, E. Martinec, and M. Wyman, *JHEP*, **09**, 087 (2013), arXiv:1305.2930.
- [77] P. Adshead, E. Martinec, and M. Wyman, *Phys. Rev.*, **D88**(2), 021302 (2013), arXiv:1301.2598.
- [78] A. Maleknejad, *JHEP*, **07**, 104 (2016), arXiv:1604.03327.
- [79] E. Dimastrogiovanni, M. Fasiello, and T. Fujita, *JCAP*, **1701**(01), 019 (2017), arXiv:1608.04216.
- [80] Fabrizio Renzi, Giovanni Cabass, Eleonora Di Valentino, Alessandro Melchiorri, and Luca Pagano, *JCAP*, **1808**(08), 038 (2018), arXiv:1803.03230.
- [81] James E. Gunn and Bruce A. Peterson, *Astrophys. J.*, **142**, 1633 (1965).
- [82] Xiao-Hui Fan et al., *Astron. J.*, **132**, 117–136 (2006), arXiv:astro-ph/0512082.
- [83] James S. Bolton et al., *Mon. Not. Roy. Astron. Soc.*, **416**, L70 (2011), arXiv:1106.6089.
- [84] Ryan Chornock, Edo Berger, Derek B. Fox, Ragnhild Lunnan, Maria R. Drout, Wen-Fai Fong, Tanmoy Laskar, and Katherine C. Roth, *Astrophys. J.*, **774**, 26 (2013), arXiv:1306.3949.
- [85] Ian McGreer, Andrei Mesinger, and Valentina D’Odorico, *Mon. Not. Roy. Astron. Soc.*, **447**(1), 499–505 (2015), arXiv:1411.5375.
- [86] G. Hinshaw et al., *Astrophys. J. Suppl.*, **208**, 19 (2013), arXiv:1212.5226.
- [87] Planck Collaboration XIII, *Astron. Astrophys.*, **594**, A13 (2016), arXiv:1502.01589.
- [88] Planck Collaboration Int. XLVI, *Astron. Astrophys.*, **596**, A107 (2016), arXiv:1605.02985.
- [89] Brant E. Robertson, Richard S. Ellis, Steven R. Furlanetto, and James S. Dunlop, *Astrophys. J.*, **802**(2), L19 (2015), arXiv:1502.02024.
- [90] Steven Furlanetto, S. Peng Oh, and Frank Briggs, *Phys. Rept.*, **433**, 181–301 (2006), arXiv:astro-ph/0608032.
- [91] Hyunbae Park, Paul R. Shapiro, Eiichiro Komatsu, Ilian T. Iliev, Kyungjin Ahn, and Garrelt Mellema, *Astrophys. J.*, **769**, 93 (2013), arXiv:1301.3607.
- [92] R. A. Sunyaev and Ya. B. Zeldovich, *Mon. Not. Roy. Astron. Soc.*, **190**, 413–420 (1980).
- [93] Planck Collaboration Int. XLVII, *Astron. Astrophys.*, **596**, A108 (2016), arXiv:1605.03507.
- [94] Matias Zaldarriaga, *Phys. Rev.*, **D55**, 1822–1829 (1997), arXiv:astro-ph/9608050.
- [95] D. N. Spergel et al., *Astrophys. J. Suppl.*, **148**, 175–194 (2003), arXiv:astro-ph/0302209.
- [96] Planck Collaboration XVI, *Astron. Astrophys.*, **571**, A16 (2014), arXiv:1303.5076.

-
- [97] J. L. Weiland, K. Osumi, G. E. Addison, C. L. Bennett, D. J. Watts, M. Halpern, and G. Hinshaw, *Astrophys. J.*, **863**, 161 (2018), arXiv:1801.01226.
- [98] Eleonora Di Valentino et al., *JCAP*, **1804**, 017 (2018), arXiv:1612.00021.
- [99] Planck Collaboration VI (2018), arXiv:1807.06209.
- [100] Erminia Calabrese, David Alonso, and Jo Dunkley, *Phys. Rev.*, **D95**(6), 063504 (2017), arXiv:1611.10269.
- [101] R. Allison, P. Caucal, E. Calabrese, J. Dunkley, and T. Louis, *Phys. Rev.*, **D92**(12), 123535 (2015), arXiv:1509.07471.
- [102] Aoife Boyle and Eiichiro Komatsu, *JCAP*, **1803**(03), 035 (2018), arXiv:1712.01857.
- [103] Julien Lesgourgues and Sergio Pastor, *Phys. Rept.*, **429**, 307–379 (2006), arXiv:astro-ph/0603494.
- [104] Amir Aghamousa et al. (2016), arXiv:1611.00036.
- [105] Paul A. Abell et al. (2009), arXiv:0912.0201.
- [106] Andreu Font-Ribera, Patrick McDonald, Nick Mostek, Beth A. Reid, Hee-Jong Seo, and An Slosar, *JCAP*, **1405**, 023 (2014), arXiv:1308.4164.
- [107] Josquin Errard, Stephen M. Feeney, Hiranya V. Peiris, and Andrew H. Jaffe, *JCAP*, **1603**(03), 052 (2016), arXiv:1509.06770.
- [108] Sophie Henrot-Versillé, Francois Couchot, Xavier Garrido, Hiroaki Imada, Thibaut Louis, Matthieu Tristram, and Sylvain Vanneste (2018), arXiv:1807.05003.
- [109] Sophie Henrot-Versillé et al., *Class. Quant. Grav.*, **32**(4), 045003 (2015), arXiv:1408.5299.
- [110] Matias Zaldarriaga, Loris Colombo, Eiichiro Komatsu, Adam Lidz, Michael Mortonson, S. Peng Oh, Elena Pierpaoli, Licia Verde, and Oliver Zahn (2008), arXiv:0811.3918.
- [111] Georges Obied, Cora Dvorkin, Chen Heinrich, Wayne Hu, and Vinicius Miranda, *Phys. Rev.*, **D98**(4), 043518 (2018), arXiv:1803.01858.
- [112] Vinicius Miranda, Adam Lidz, Chen He Heinrich, and Wayne Hu, *Mon. Not. Roy. Astron. Soc.*, **467**(4), 4050–4056 (2017), arXiv:1610.00691.
- [113] Rennan Barkana and Abraham Loeb, *Rept. Prog. Phys.*, **70**, 627 (2007), arXiv:astro-ph/0611541.
- [114] Steven Furlanetto and Abraham Loeb, *Astrophys. J.*, **634**, 1–13 (2005), arXiv:astro-ph/0409656.
- [115] A. Roy, A. Lapi, D. Spergel, and C. Baccigalupi, *JCAP*, **1805**(05), 014 (2018), arXiv:1801.02393.
- [116] Shun Saito, Kiyotomo Ichiki, and Atsushi Taruya, *JCAP*, **0709**, 002 (2007), arXiv:0705.3701.
- [117] Sean M. Carroll, *Phys. Rev. Lett.*, **81**, 3067–3070 (1998), arXiv:astro-ph/9806099.
- [118] Arthur Lue, Li-Min Wang, and Marc Kamionkowski, *Phys. Rev. Lett.*, **83**, 1506–1509 (1999), arXiv:astro-ph/9812088.
- [119] Planck Collaboration Int. XLIX, *Astron. Astrophys.*, **596**, A110 (December 2016).
- [120] D. Molinari, A. Gruppuso, and P. Natoli, *Physics of the Dark Universe*, **14**, 65–72 (December 2016), 1605.01667.
- [121] Bo Feng, Hong Li, Ming-zhe Li, and Xin-min Zhang, *Phys. Lett.*, **B620**, 27–32 (2005), arXiv:hep-ph/0406269.
- [122] Brian Keating, Meir Shimon, and Amit Yadav, *Astrophys. J.*, **762**, L23 (2012), arXiv:1211.5734.
- [123] Mingzhe Li and Xinmin Zhang, *Phys. Rev.*, **D78**, 103516 (2008), arXiv:0810.0403.
- [124] Maxim Pospelov, Adam Ritz, and Constantinos Skordis, *Phys. Rev. Lett.*, **103**, 051302 (2009), arXiv:0808.0673.
- [125] Marc Kamionkowski, *Phys. Rev. Lett.*, **102**, 111302 (2009), arXiv:0810.1286.
- [126] Toshiya Namikawa, *Phys. Rev.*, **D95**(4), 043523 (2017), arXiv:1612.07855.
- [127] Peter A. R. Ade et al., *Phys. Rev.*, **D92**, 123509 (2015), arXiv:1509.02461.
- [128] P. A. R. Ade et al., *Phys. Rev.*, **D96**(10), 102003 (2017), arXiv:1705.02523.
- [129] Ya. B. Zeldovich and R. A. Sunyaev, *Astrophys. Space Sci.*, **4**, 301–316 (1969).
- [130] R. A. Sunyaev and Ya. B. Zeldovich, *Comments Astrophys. Space Phys.*, **4**, 173–178 (1972).
- [131] John E. Carlstrom, Gilbert P. Holder, and Erik D. Reese, *Ann. Rev. Astron. Astrophys.*, **40**, 643–680 (2002), arXiv:astro-ph/0208192.
- [132] L. E. Bleem et al., *Astrophys. J. Suppl.*, **216**(2), 27 (2015), arXiv:1409.0850.
- [133] Planck Collaboration XXVII, *Astron. Astrophys.*, **594**, A27 (2016), arXiv:1502.01598.
- [134] Matt Hilton et al., *Astrophys. J. Suppl.*, **235**(1), 20 (2018), arXiv:1709.05600.
- [135] M. Remazeilles, J. Delabrouille, and J.-F. Cardoso, *Mon. Not. Roy. Astron. Soc.*, **410**, 2481–2487 (2011), arXiv:1006.5599.
- [136] M. Remazeilles, N. Aghanim, and M. Douspis, *Mon. Not. Roy. Astron. Soc.*, **430**, 370–385 (2013), arXiv:1207.4683.
- [137] Planck Collaboration XXII, *Astron. Astrophys.*, **594**, A22 (2016), arXiv:1502.01596.
- [138] Ryu Makiya, Shin'ichiro Ando, and Eiichiro Komatsu, *Mon. Not. Roy. Astron. Soc.* (2018), arXiv:1804.05008.
- [139] J. Colin Hill, Nick Battaglia, Jens Chluba, Simone Ferraro, Emmanuel Schaan, and David N. Spergel, *Phys. Rev. Lett.*, **115**(26), 261301 (2015), arXiv:1507.01583.

-
- [140] C. Burigana, L. Danese, and G. de Zotti, *Astron. Astrophys.*, **246**, 49–58 (June 1991).
- [141] Wayne Hu and Joseph Silk, *Phys. Rev.*, **D48**, 485–502 (1993).
- [142] Hiroyuki Tashiro, *PTEP*, **2014**(6), 06B107 (2014).
- [143] Jens Chluba, Jan Hamann, and Subodh P. Patil, *Int. J. Mod. Phys.*, **D24**(10), 1530023 (2015), arXiv:1505.01834.
- [144] Joseph Silk, *Astrophys. J.*, **151**, 459–471 (1968).
- [145] R. A. Sunyaev and Y. B. Zeldovich, *Astrophys. Space Sci.*, **9**, 368–382 (1970).
- [146] R. A. Daly, *Astrophys. J.*, **371**, 14–28 (1991).
- [147] J. D. Barrow and P. Coles, *Mon. Not. Roy. Astron. Soc.*, **248**, 52–57 (1991).
- [148] Wayne Hu, Douglas Scott, and Joseph Silk, *Astrophys. J.*, **430**, L5–L8 (1994), arXiv:astro-ph/9402045.
- [149] Enrico Pajer and Matias Zaldarriaga, *Phys. Rev. Lett.*, **109**, 021302 (2012), arXiv:1201.5375.
- [150] Jonathan Ganc and Eiichiro Komatsu, *Phys. Rev.*, **D86**, 023518 (2012), arXiv:1204.4241.
- [151] Planck Collaboration XVII, *Astron. Astrophys.*, **594**, A17 (2016), arXiv:1502.01592.
- [152] Suvodip Mukherjee, Rishi Khatri, and Benjamin D. Wandelt, *JCAP*, **1804**, 045 (2018), arXiv:1801.09701.
- [153] Planck Collaboration XVI, *Astron. Astrophys.*, **594**, A16 (2016), arXiv:1506.07135.
- [154] Planck Collaboration I (2018), arXiv:1807.06205.
- [155] Planck Collaboration XXIII, *Astron. Astrophys.*, **571**, A23 (2014), arXiv:1303.5083.
- [156] H. K. Eriksen, F. K. Hansen, A. J. Banday, K. M. Gorski, and P. B. Lilje, *Astrophys. J.*, **605**, 14–20, [Erratum: *Astrophys. J.* 609, 1198 (2004)] (2004), arXiv:astro-ph/0307507.
- [157] Hans K. Eriksen, A. J. Banday, K. M. Gorski, F. K. Hansen, and P. B. Lilje, *Astrophys. J.*, **660**, L81–L84 (2007), arXiv:astro-ph/0701089.
- [158] A. Gruppuso, N. Kitazawa, M. Lattanzi, N. Mandolesi, P. Natoli, and A. Sagnotti, *Phys. Dark Univ.*, **20**, 49–64 (2018), arXiv:1712.03288.
- [159] Kate Land and Joao Magueijo, *Phys. Rev. Lett.*, **95**, 071301 (2005), arXiv:astro-ph/0502237.
- [160] Adam G. Riess et al., *Astrophys. J.*, **826**(1), 56 (2016), arXiv:1604.01424.
- [161] A. Brandenburg and K. Subramanian, *Phys. Rept.*, **417**, 1–209 (October 2005), astro-ph/0405052.
- [162] Planck Collaboration XI, *Astron. Astrophys.* in press (2018), 1801.04945.
- [163] J. Chluba, J. C. Hill, and M. H. Abitbol, *Mon. Not. Roy. Astron. Soc.*, **472**, 1195–1213 (November 2017), 1701.00274.
- [164] V. Jelić, S. Zaroubi, P. Labropoulos, G. Bernardi, A. G. de Bruyn, and L. V. E. Koopmans, *Mon. Not. Roy. Astron. Soc.*, **409**, 1647–1659 (December 2010), 1007.4135.
- [165] S. A. Mao, C. Carilli, B. M. Gaensler, O. Wucknitz, C. Keeton, A. Basu, R. Beck, P. P. Kronberg, and E. Zweibel, *Nature Astronomy*, **1**, 621–626 (August 2017), 1708.07844.
- [166] G. Giacinti, M. Kachelrieß, D. V. Semikoz, and G. Sigl, *Astroparticle Physics*, **35**, 192–200 (November 2011), arXiv:1104.1141.
- [167] F. Boulanger et al., *JCAP*, **8**, 049 (August 2018), 1805.02496.
- [168] Planck Collaboration I, *Astron. Astrophys.*, **594**, A1 (2016), 1502.01582.
- [169] Planck Collaboration XII, *Astron. Astrophys.* submitted (2018), 1807.06212.
- [170] Tassis, K. et al., *ArXiv e-prints* (October 2018), arXiv:1810.05652.
- [171] Haverkorn, M. et al., *Advancing Astrophysics with the Square Kilometre Array (AASKA14)*, page 96 (April 2015), 1501.00416.
- [172] P. Hennebelle and E. Falgarone, *Astron. Astrophys. Rev.*, **20**, 55 (November 2012), 1211.0637.
- [173] Planck Collaboration Int. XXXII, *Astron. Astrophys.*, **586**, A135 (2016), 1409.6728.
- [174] Planck Collaboration Int. XXXV, *Astron. Astrophys.*, **586**, A138 (February 2016), 1502.04123.
- [175] S. L. Wilkin, C. F. Barenghi, and A. Shukurov, *Phys. Rev. Letters*, **99**(13), 134501 (September 2007), astro-ph/0702261.
- [176] G. Momferratos, P. Lesaffre, E. Falgarone, and G. Pineau des Forêts, *Mon. Not. Roy. Astron. Soc.*, **443**, 86–101 (September 2014), 1502.03624.
- [177] C. Federrath, *Journal of Plasma Physics*, **82**(6), 535820601 (December 2016), arXiv:1610.08132.
- [178] Planck Collaboration IV, *Astron. Astrophys.* submitted (2018), 1807.06208.
- [179] B. T. Draine and B. Hensley, *Astrophys. J.*, **765**, 159 (March 2013), 1205.7021.
- [180] C. Dickinson et al., *New Astron. Rev.*, **80**, 1–28 (February 2018), 1802.08073.
- [181] Planck Collaboration Int. XXII, *Astron. Astrophys.*, **576**, A107 (2015), 1405.0874.
- [182] M. E. Jones et al., *Mon. Not. Roy. Astron. Soc.*, **480**, 3224–3242 (November 2018), arXiv:1805.04490.
- [183] Planck Collaboration XI, *Astron. Astrophys.*, **571**, A11 (2014), 1312.1300.
- [184] Planck Collaboration Int. XVII, *Astron. Astrophys.*, **566**, A55 (2014), 1312.5446.
- [185] T. Hoang and A. Lazarian, *Astrophys. J.*, **831**, 159 (November 2016), 1605.02828.